Supporting information

Computation-aided redesign of C-glycosyltransferases facilitates sustainable biosynthesis of C-glycosides

Xinhe Liu[a], Jialin Li[a], Wenrui Zhao[a], Xuesong Gong[a], Qiuyan Sun[a], Xudong Feng[a*]

and Chun Li[b, c, d, e*]

[a]Key Laboratory of Medical Molecule Science and Pharmaceutical Engineering, Ministry of Industry and Information Technology, Institute of Biochemical Engineering, School of Chemistry and Chemical Engineering, Beijing Institute of Technology, Beijing 100081, China

[b]Key Lab for Industrial Biocatalysis, Ministry of Education, Department of Chemical Engineering, Tsinghua University, Beijing 100084, China

[c]Center for Synthetic and Systems Biology, Tsinghua University, Beijing 100084, China

[d]Beijing Key Laboratory of Recombinant Protein Synthetic Biomanufacturing, Beijing 100084, China

[e]State Key Laboratory of Green Biomanufacturing, Beijing 100084, China

[*]Correspondence to Xudong Feng (xd.feng@bit.edu.cn), Chun Li (lichun@tsinghua.edu.cn)

Supplementary Figures

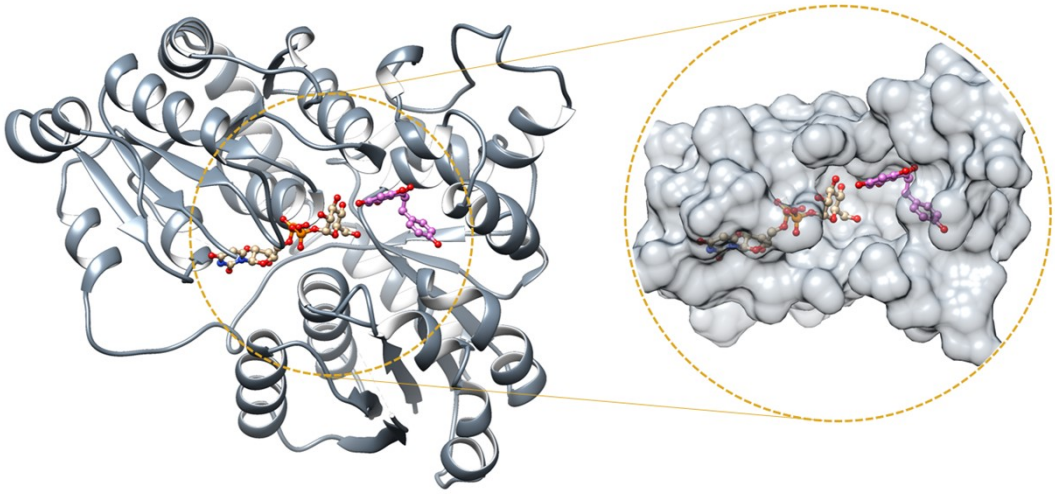

Fig. S1 Active pocket in the protein structure of UGT708B4 WT (PDB ID: 6L5P). Protein is represented as the grey ribbon. UDP-Glc is represented as the light gold stick. Phloretin is represented as the orchid stick.

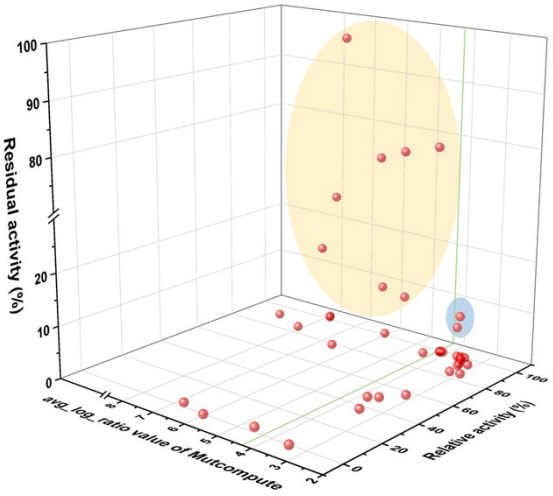

Fig. S2 Statistical analysis of mutant prediction and thermostability classification. Mutant predictions were based on avg_log_ratio values calculated using MutCompute. Experimental characterization included measurements of relative activity and residual activity. Red dots represent experimentally characterized mutants. The green line indicates the boundary between the high-score group (19 mutants) and the low-score group (19 mutants), defined by an avg_log_ratio threshold of 4.24. The yellow and blue regions represent mutants with improved thermostability in the high-score group (8 mutants) and the low-score group (2 mutants), respectively.

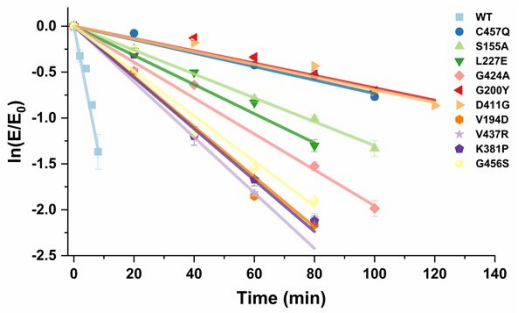

Fig. S3 The first-order kinetics fitting of thermal deactivation of UGT708B4 WT and mutants C457Q, G424A, L227E, S155A, G200Y, D411G, V194D, V437R, K381P and G456S at 50 °C. Error bars represent the mean ± standard deviation (n=3).

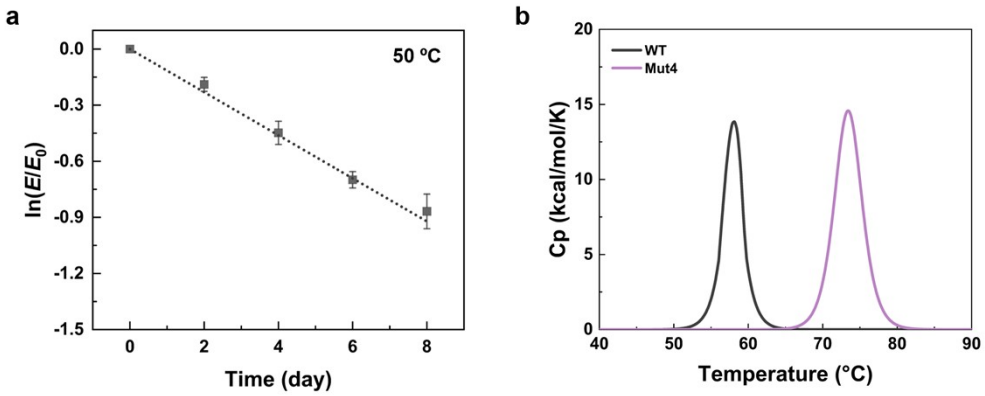

Fig. S4 Thermostability characterization of Mut4. (a) The first-order kinetics fitting of thermal deactivation at 50 °C. (b) DSC scanning curve. Error bars represent the mean ± standard deviation (n=3).

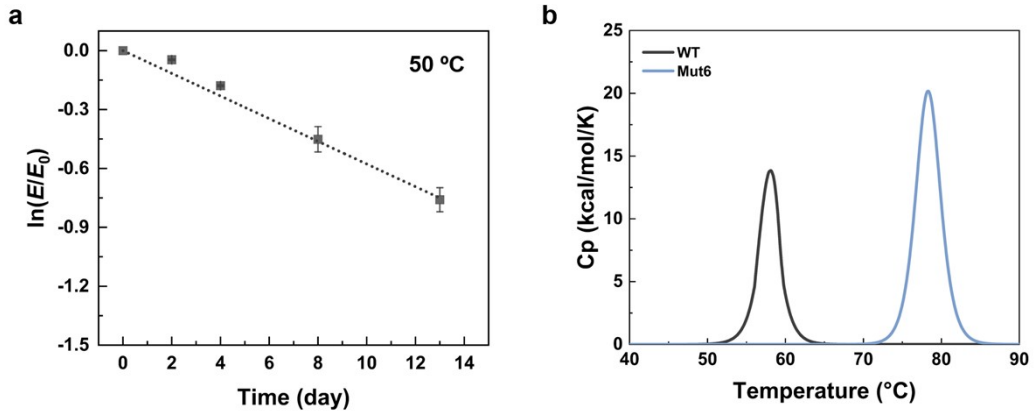

Fig. S5 Thermostability characterization of Mut6. (a) The first-order kinetics fitting of thermal deactivation at 50 °C. (b) DSC scanning curve. Error bars represent the mean ± standard deviation (n=3).

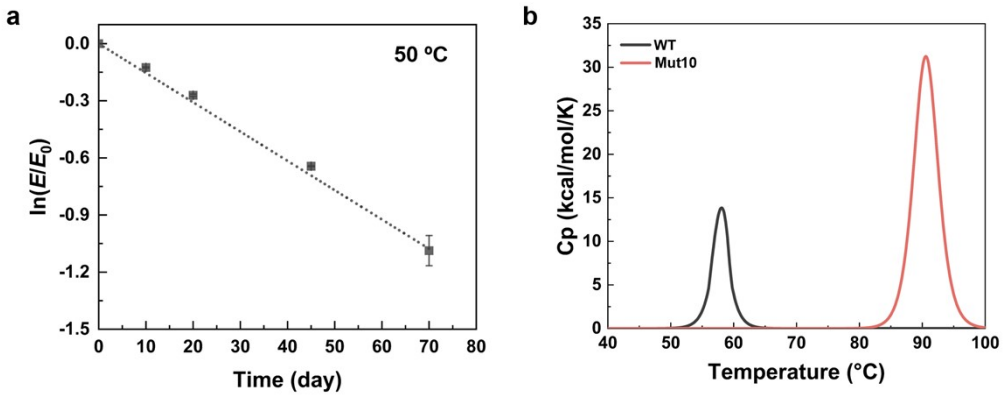

Fig. S6 Thermostability characterization of Mut10. (a) The first-order kinetics fitting of thermal deactivation at 50 °C. (b) DSC scanning curve. Error bars represent the mean ± standard deviation (n=3).

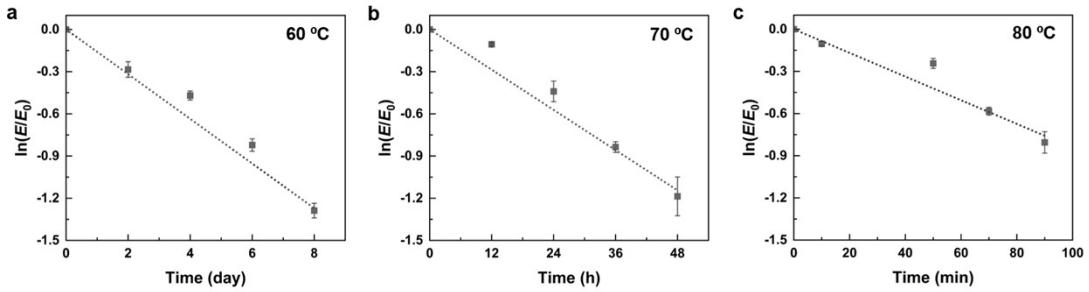

Fig. S7 The first-order kinetics fitting of thermal deactivation of Mut10 at 60 °C (a), 70 °C (b) and 80 °C (c). Error bars represent the mean ± standard deviation (n=3).

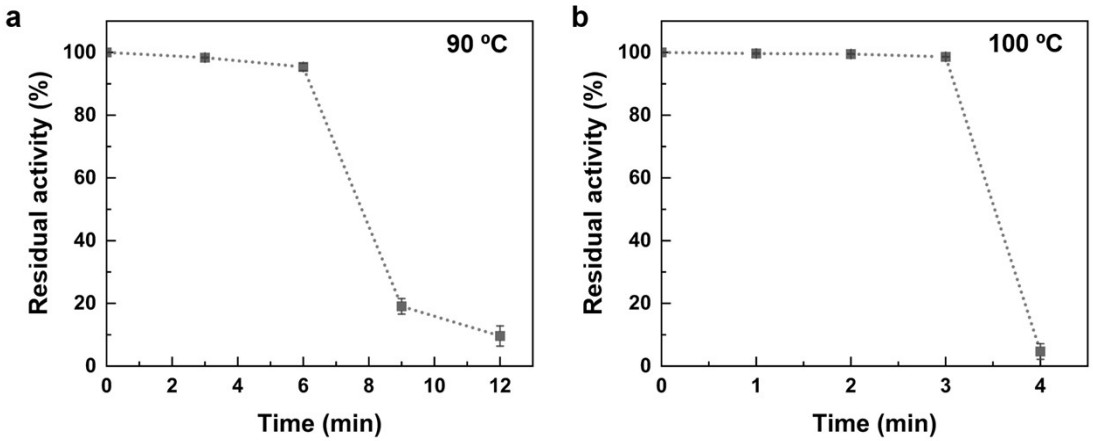

Fig. S8 Thermostability of Mut10 at 90 °C (a) and 100 °C (b). Error bars represent the mean ± standard deviation (n=3).

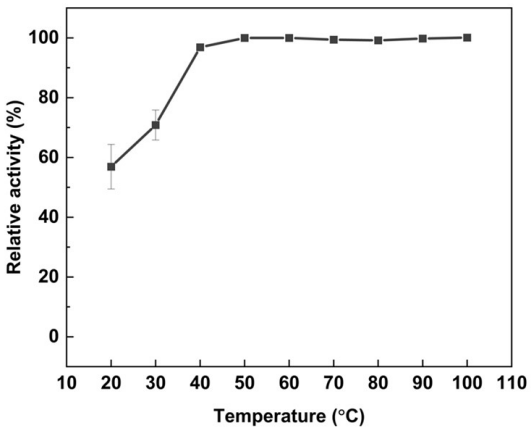

Fig. S9 Temperature profile of Mut10. Error bars represent the mean ± standard deviation (n=3).

Fig. S10 pH profile of Mut10. Different reaction buffers: pH 3.0−6.0 (citric acid-sodium citrate buffer), pH 6.0−8.0 (Na_2HPO_4-NaH_2PO_4 buffer), pH 8.0−9.0 (Tirs-HCl buffer), and pH 10.0−11.0 (Na_2CO_3-$NaHCO_3$ buffer). Error bars represent the mean ± standard deviation (n=3).

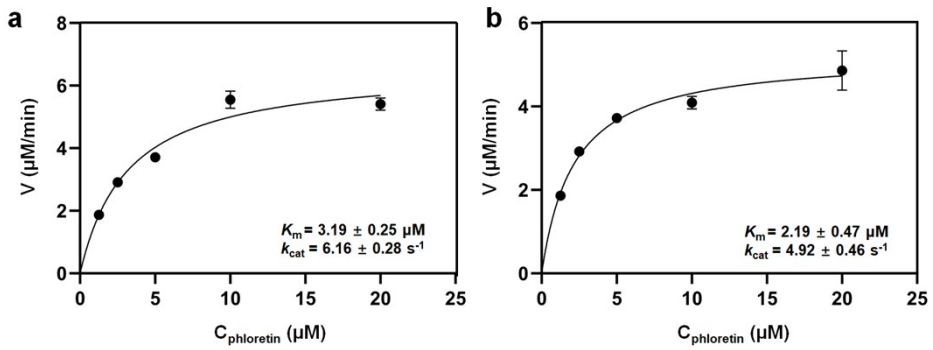

Fig. S11 Michaelis-Menten kinetics of WT (a) and Mut10 (b). Error bars represent the mean ± standard deviation (n=3).

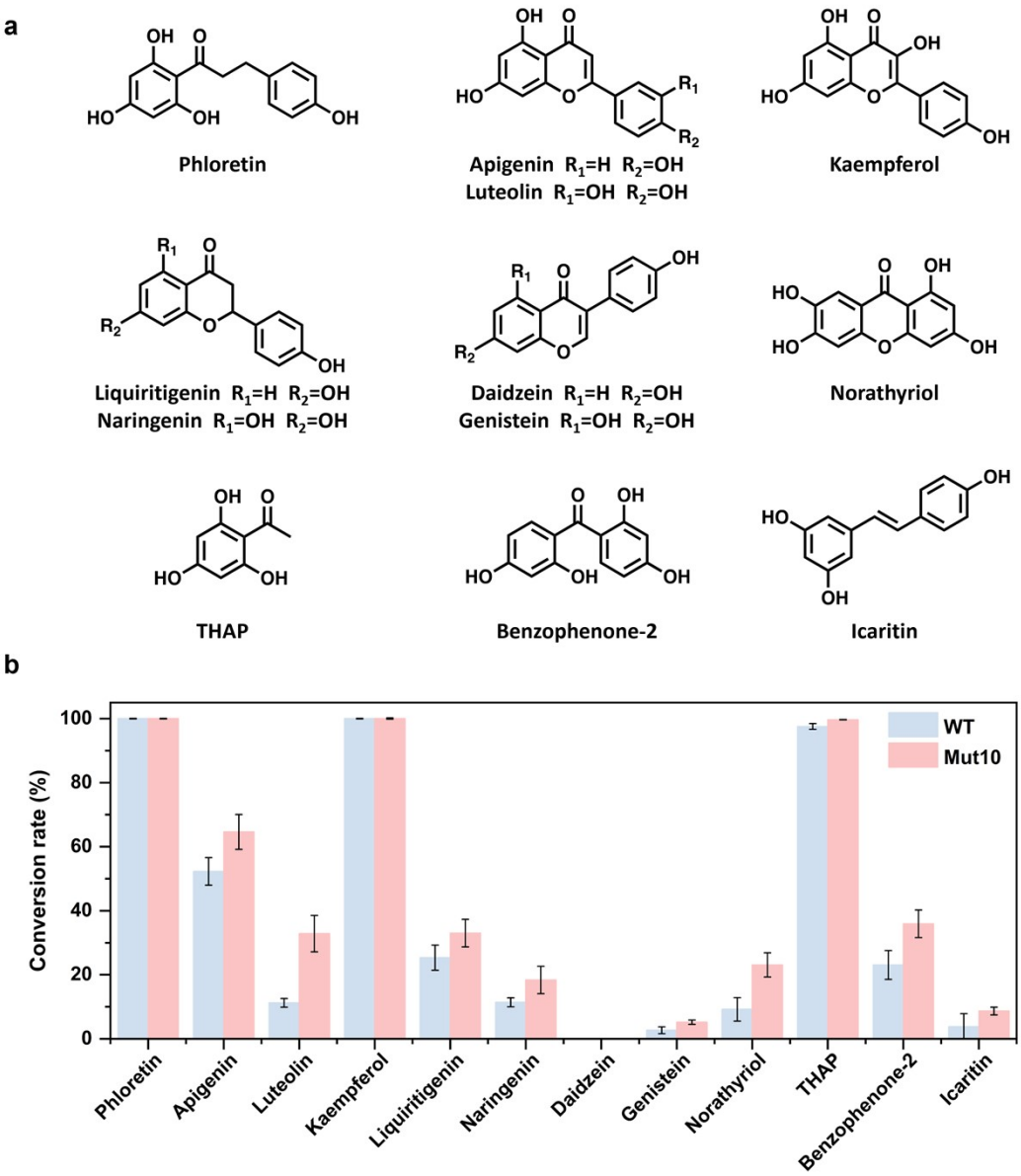

Fig. S12 Substrate scope characterization. (a) Chemical structures of compounds used as sugar acceptors. (b) Substrate scope of WT and Mut10. UDP-Glc was used as the sugar donor. Error bars represent the mean ± standard deviation (n=3).

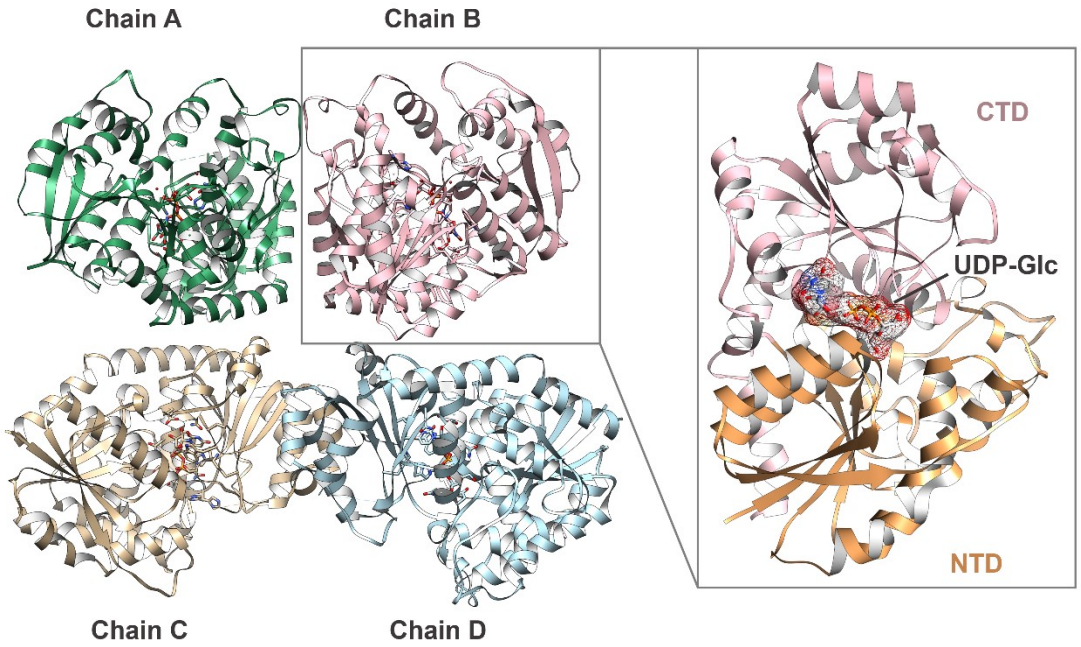

Fig. S13 The crystal structure of Mut10. Each asymmetric unit of Mut10 contained four chains.

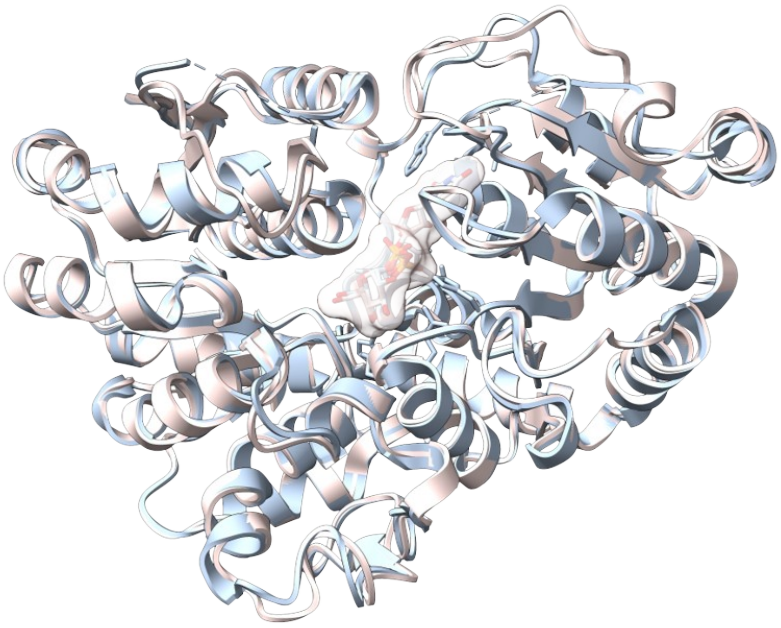

Fig. S14 Structure superposition of WT (blue) and Mut10 (pink). The protein is represented as the ribbon in different colors. UDP-Glc is represented as the stick with surface.

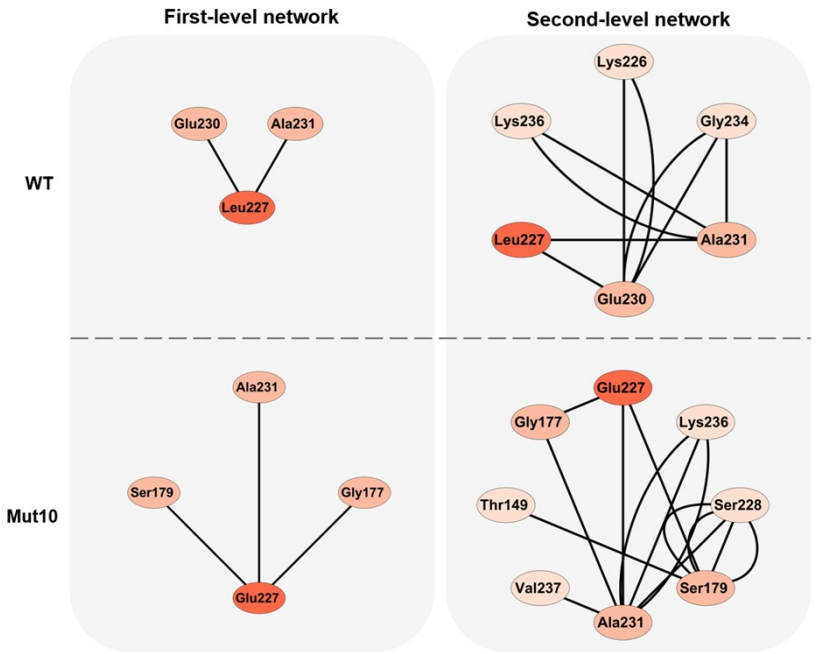

Fig. S15 The first-level network and second-level network based on node 227 in WT and Mut10.

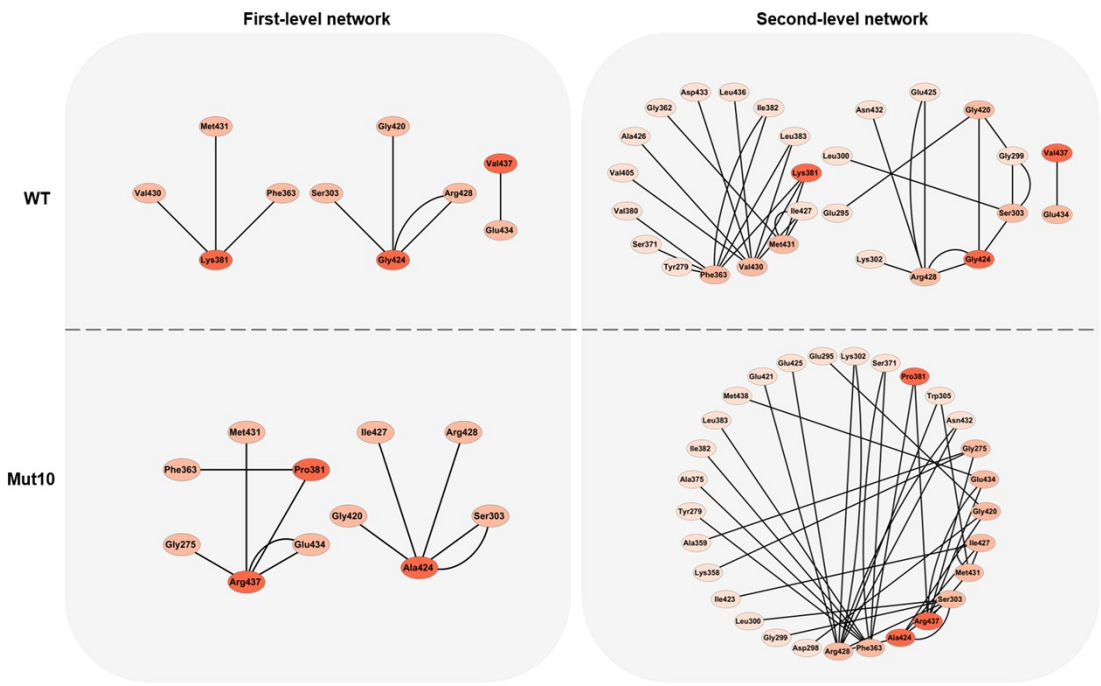

Fig. S16 The first-level network and second-level network based on node 381, 424 and 437 in WT and Mut10.

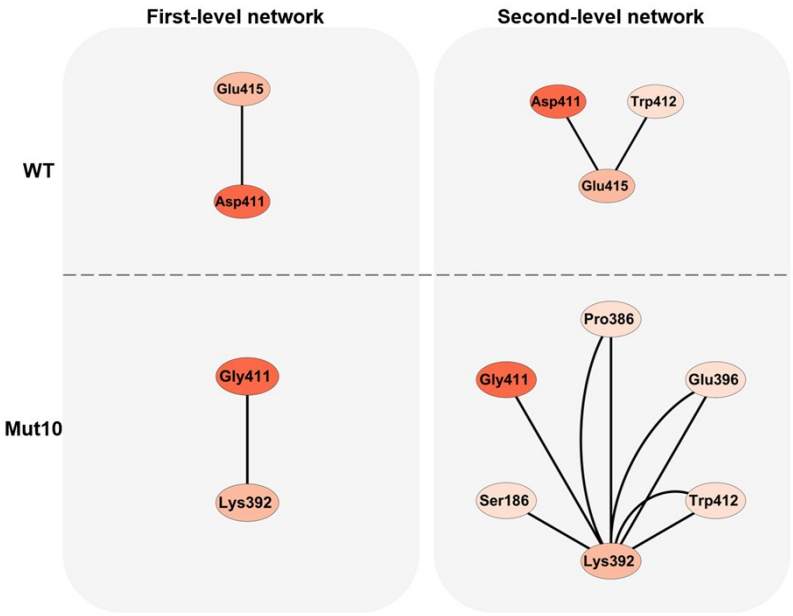

Fig. S17 The first-level network and second-level network based on node 411 in WT and Mut10.

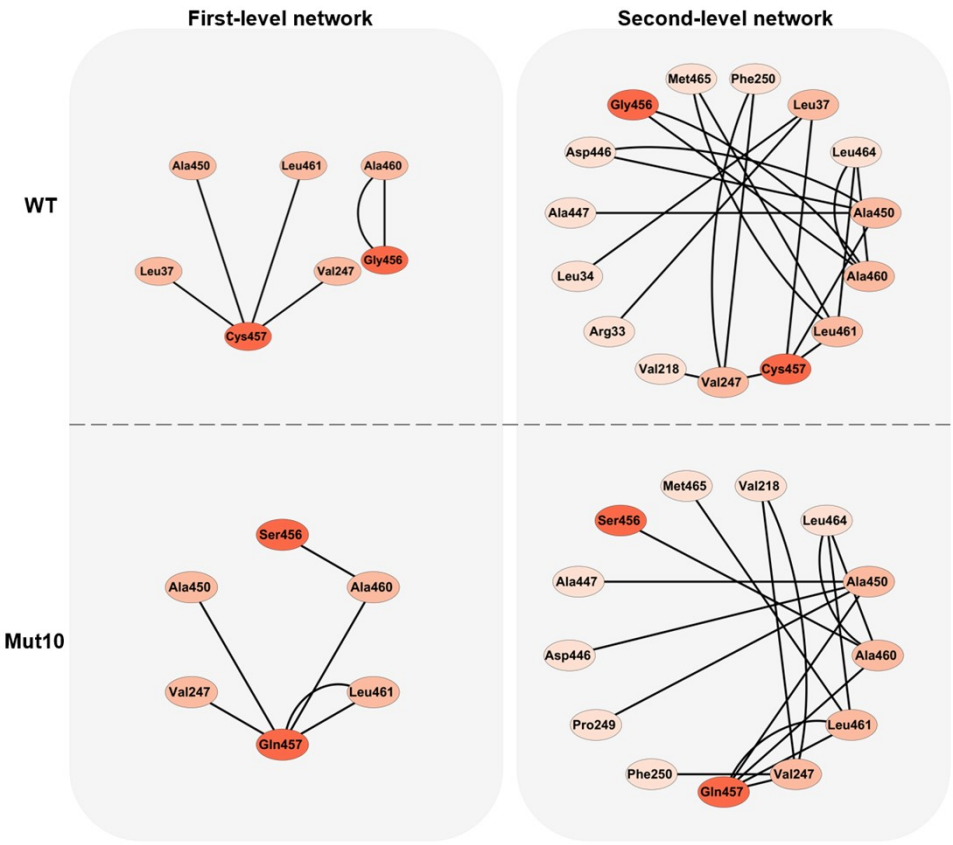

Fig. S18 The first-level network and second-level network based on node 456 and 457 in WT and Mut10.

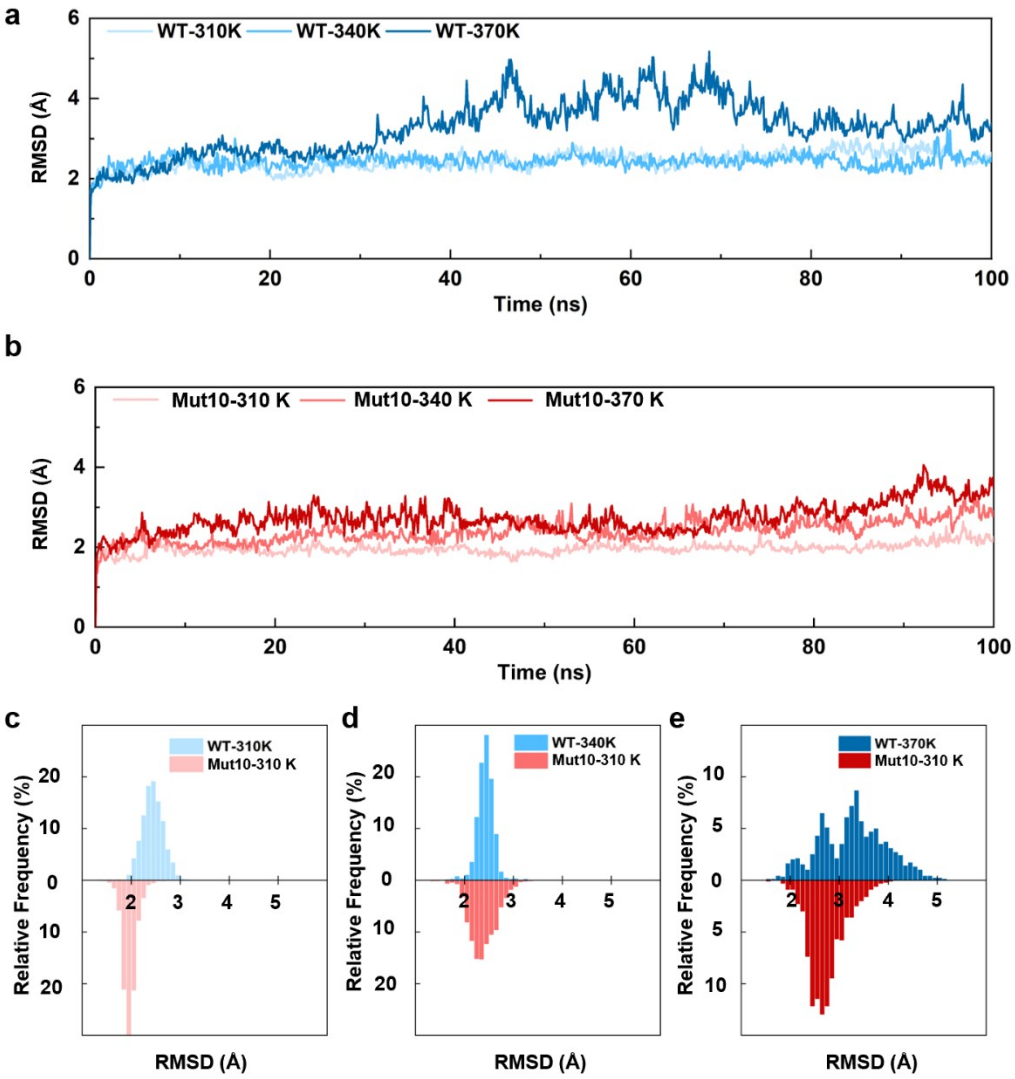

Fig. S19 RMSD analysis based on 100 ns MD simulation. RMSD of WT (a) and Mut10 (b) at different temperatures. Relative frequency histograms of RMSD value of WT and Mut10 at 310 K (c), 340 K (d) and 370 K (e).

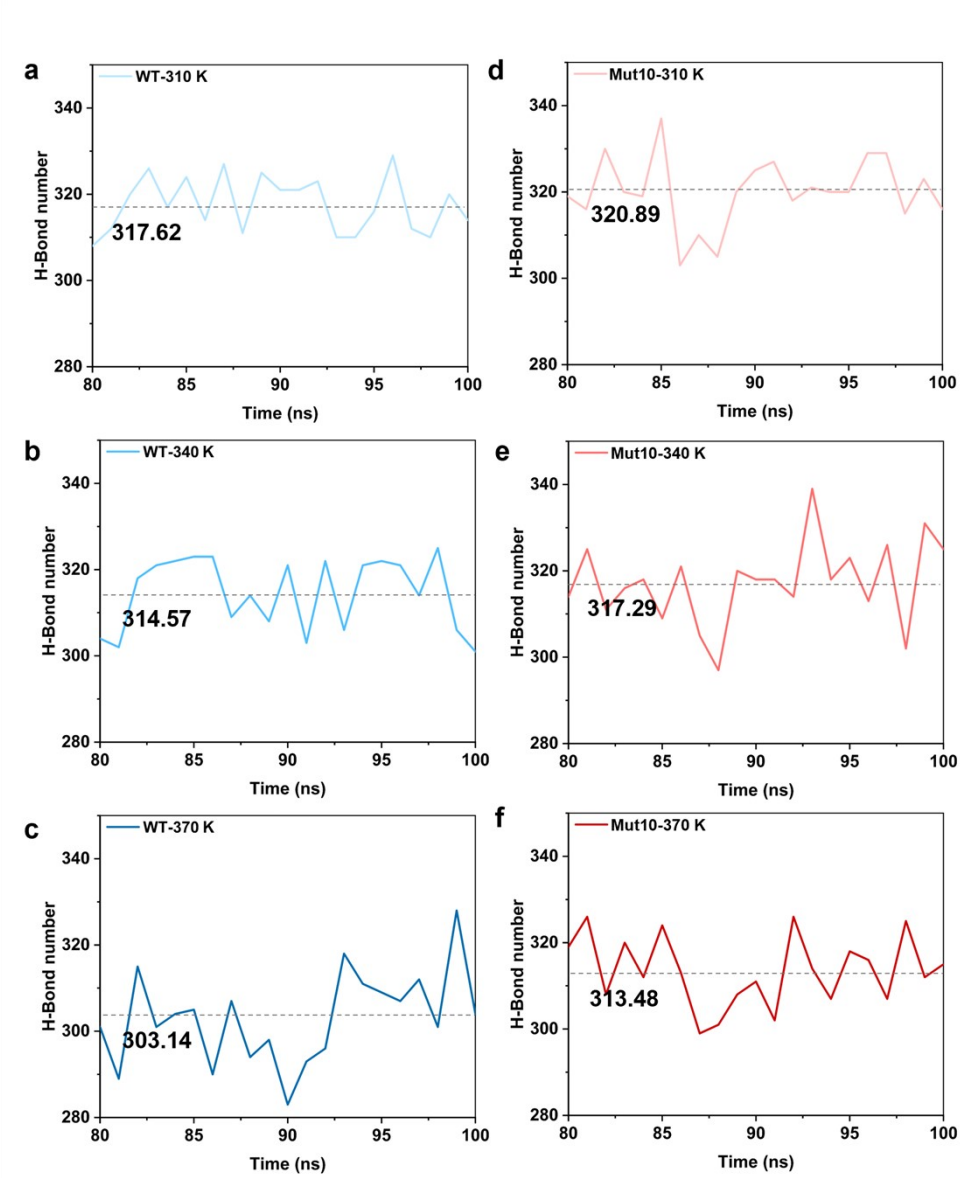

Fig. S20 Overall hydrogen bonds analysis in WT (a−c) and Mut10 (d−f) over the final 20 ns of MD simulations. Overall hydrogen bonds analysis of WT at 310 K (a), 340 K (b) and 370 K (c). Overall hydrogen bonds analysis of Mut10 at 310 K (d), 340 K (e) and 370 K (f).

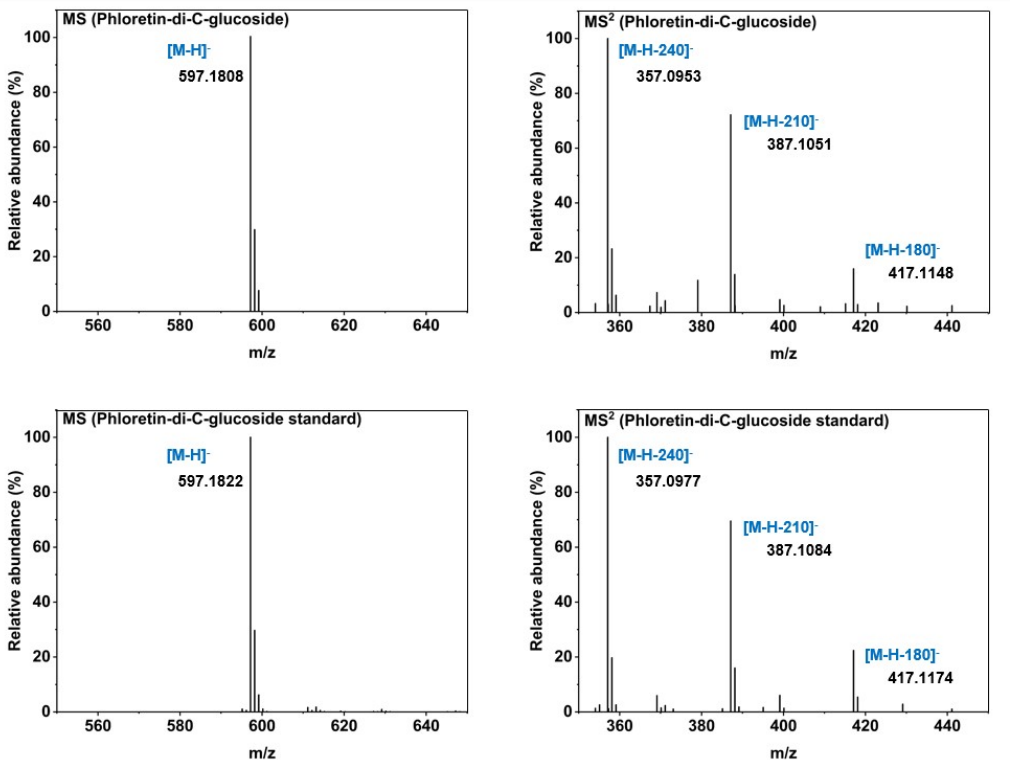

Fig. S21 LC-MS/MS analysis of the product phloretin di-C-glucoside and the standard.

Supplementary Tables

Table S1 The residues constituting the active pocket of UGT708B4 WT analyzed by ProteinPlus.

Residues
Gly24−His27, Thr29，Pro30，Arg33，Phe92，Phe95，Arg99， Met123-Leu125，Phe144−Ser146，Met150，Phe153，Phe154， Pro189-Leu192，Leu198，Phe199，Leu202，Phe203，Asp206，Glu256， Tyr279，Ser281−Thr286，Val310，Lys312，Glu347−Ser352，Leu355， Ser365−Val372，Glu374，His388−Gln391，Asn394

Table S2 Mutations predicted by MutCompute.

Mutants	avg_log_ratio	Mutants	avg_log_ratio
Q51V	14.07	S22N	4.22
E415V	8.06	S36A	4.16
K211P	7.95	D350Q	4.08
K346N	7.81	D446S	3.84
V180P	7.66	L129M	3.75
V259P	7.61	L104N	3.73
C457Q	7.34	S181D	3.63
S284T	7.04	R290K	3.62
V459Q	6.86	S187C	3.59
E458K	6.49	T49V	3.57
G424A	6.21	T441S	3.54
S97A	6.11	M438E	3.52
F172V	6.06	E267K	3.52
S163D	6.01	S165D	3.51
L227E	5.48	S111N	3.50
F330E	5.40	S102A	3.41
K312F	5.15	K201S	3.36
T264A	4.70	T106L	3.28
D313A	4.51	C43N	3.22
S155A	4.44	V238T	3.20
S274A	4.25	N370Q	3.10
H40E	4.24	E353L	3.01

Table S3 $t_{1/2}$ of mutants (50 °C).

Mutants	k_d	$t_{1/2}$	Fold
WT	0.156 ± 0.0149 min^{-1}	4.48 ± 0.40 min	/
C457Q	0.007 ± 0.0002 min^{-1}	94.14 ± 2.15 min	21.15 ± 1.57
S155A	0.013 ± 0.0003 min^{-1}	53.76 ± 1.21 min	12.12 ± 1.36
L227E	0.015 ± 0.0005 min^{-1}	46.37 ± 1.66 min	10.45 ± 1.17
G424A	0.019 ± 0.0006 min^{-1}	36.19 ± 1.07 min	8.14 ± 0.66
G200Y	0.006 ± 0.0001 min^{-1}	108.31 ± 1.38 min	24.39 ± 2.39
D411G	0.007 ± 0.0001 min^{-1}	104.00 ± 1.96 min	23.42 ± 2.25
V194D	0.028 ± 0.0005 min^{-1}	24.59 ± 0.43 min	5.54 ± 0.59
V437R	0.028 ± 0.0004 min^{-1}	24.64 ± 0.36 min	5.56 ± 0.61
K381P	0.028 ± 0.0009 min^{-1}	25.23 ± 0.82 min	5.69 ± 0.67
G456S	0.025 ± 0.0007 min^{-1}	28.04 ± 0.77 min	6.31 ± 0.58
Mut4	0.111 ± 0.0039 d^{-1}	6.26 ± 0.22 d	2022.83 ± 129.38
Mut6	0.056 ± 0.0044 d^{-1}	12.35 ± 0.91 d	4011.73 ± 156.06
Mut10	0.015 ± 0.0007 d^{-1}	46.22 ± 2.33 d	15057.12 ± 433.70

Table S4 The energy value of mutants predicted by FireProt.

Mutants	FoldX (kcal/mol)	Rosetta (kcal/mol)
E339L	-1.00	-17.34
V467M	-1.04	-7.65
G200W	-2.16	-7.44
G246P	-2.01	-7.26
C253F	-2.05	-5.06
S179F	-1.62	-4.95
T49V	-1.14	-3.4
S207A	-1.61	-3.4
T106Y	-1.85	-3.08
D411G	-1.62	-2.99
F330P	-1.42	-2.88
Q51I	-1.67	-2.54
S274P	-1.23	-2.48
S110L	-1.59	-2.48
T53P	-1.96	-2.2
V333W	-2.07	-2.08

Table S5 Mutations predicted by PROSS.

Mutants			
V437R	K445E	V194N	G424A
T106A/H	K381P	S36A/V	D206N
S207A	G456S	S155A/L	V430M
S118A	G409E	S102A	V218I
S100A	G289S	M438E	H140C
P191L/F	G200Y	E59S	S197H
P128C/T	D446E	V459K	H44Q
L227E/R	D411G	K358P	G223A
L20F	P208R	H214D	V296L

Table S6 Mutations predicted by Consensus Finder.

Mutants	Score (%)	Mutants	Score (%)	Mutants	Score (%)
C457S	88	V194D	61	N432E	39
K381P	86	M336T	59	S352V	37
F250L	78	A399E	59	M438E	35
S118A	77	A319E	55	M465I	35
V301E	76	W403L	54	K169L	33
V437R	74	K445E	54	G246C	33
G384A	74	V373L	52	W305Q	33
G456S	74	V296I	51	L227E	31
G289S	71	E339K	48	V467S	31
I224L	70	K226P	48	G326E	30
S266L	67	D411G	45	K407V	29
P80L	66	F330E	45	H214D	28
V333L	66	E59S	44	E164T	26
V337K	62	S100R	41	G200T	25
A96E	62	D446E	41	H140T	20

Table S7 Crystallographic data collection and refinement statistics for Mut10/UDP-Glc (PDB ID: 8ZNM).

Parameters	Mut10/UDP-Glc
Data collection	
Wavelength	0.97915
Space group	P 1
Cell dimensions	
a, *b*, *c* (Å)	75.618, 81.849, 94.141
α, *β*, *γ* (°)	64.760, 88.281, 88.244
Resolution (Å)	29.64−2.21 (2.289−2.21)
R_{merge}	0.05923 (0.4958)
$I / \sigma I$	7.54 (2.65)
Completeness (%)	96.75 (97.15)
Redundancy	3.5 (3.4)
Refinement	
No. reflections (overall)	98868 (9933)
No. reflections (test set)	5169 (508)
R_{work} / R_{free}	0.1764 / 0.2174
No. atoms	
Macromolecules	14045
Ligand	144
Solvent	528
B-factor	
Macromolecules (Å^2)	52.97
Ligand (Å^2)	49.48
Solvent (Å^2)	38.40
R. m. s. deviations	
Bond lengths (Å)	0.003
Bond angles (°)	0.580

Table S8 Interaction analysis of WT based on first-level network.

Node-Node	Interaction	Node-Node	Interaction
Phe151-Ser155	H-bond	Lys381-Val430	H-bond
Ser155-Pro158	vdWs	Lys381-Met431	vdWs
Ser155-Val238	vdWs	Asp411-Glu415	vdWs
Ser155-Val238	vdWs	Gly420-Gly424	H-bond
Ser197-Gly200	vdWs	Gly424-Arg428	H-bond
Gly200-Met204	vdWs	Gly424-Arg428	vdWs
Leu227-Glu230	H-bond	Glu434-Val437	H-bond
Leu227-Ala231	H-bond	Ala450-Cys457	H-bond
Val247-Cys457	vdWs	Gly456-Ala460	H-bond
Ser303-Gly424	vdWs	Gly456-Ala460	vdWs
Phe363-Lys381	vdWs	Cys457-Leu461	H-bond
Leu37-Cys457	vdWs		

Table S9 Interaction analysis of Mut10 based on first-level network.

Node-Node	Interaction	Node-Node	Interaction
Phe151-Ala155	H-bond	Gly275-Arg437	H-bond
Phe157-Tyr200	π-π stacking	Ser303-Ala424	vdWs
Phe166-Tyr200	π-π stacking	Ser303-Ala424	vdWs
Gly177-Glu227	vdWs	Phe363-Pro381	H-bond
Ser179-Glu227	vdWs	Pro381-Arg437	vdWs
Pro191-Asp194	H-bond	Lys392-Gly411	vdWs
Pro191-Asp194	vdWs	Gly420-Ala424	H-bond
Asp194-Ser197	H-bond	Ala424-Ile427	vdWs
Asp194-Ser197	vdWs	Ala424-Arg428	H-bond
Asp194-Tyr200	vdWs	Met431-Arg437	H-bond
Pro195-Tyr200	vdWs	Glu434-Arg437	vdWs
Pro195-Tyr200	vdWs	Glu434-Arg437	vdWs
Ser197-Tyr200	vdWs	Ala450-Gln457	H-bond
Tyr200-Met204	H-bond	Ser456-Ala460	H-bond
Tyr200-Met204	vdWs	Gln457-Ala460	vdWs
Glu227-Ala231	H-bond	Gln457-Leu461	H-bond
Val247-Gln457	H-bond	Gln457-Leu461	vdWs

Table S10 The number of interactions between different edge types of WT and Mut10 based on first-level network.

Interaction	WT	Mut10
H-bond	10	14
π-π stacking	0	2
π-cation	0	0
Ionic bond	0	0
π-H bond	0	0
vdWs	13	18
Total number	23	34

Table S11 Interaction analysis of WT based on second-level network.

Node-Node	Interaction	Node-Node	Interaction
Arg33-Leu37	H-bond	Gly299-Gly420	vdWs
Leu34-Leu37	vdWs	Leu300-Ser303	vdWs
Leu37-Cys457	vdWs	Lys302-Arg428	H-bond
Phe144-Phe151	π-π stacking	Ser303-Gly424	vdWs
Ser147-Phe151	H-bond	Gly362-Met431	vdWs
Ala148-Phe151	vdWs	Phe363-Ser371	vdWs
Phe151-Phe154	π-π stacking	Phe363-Val380	vdWs
Phe151-Phe154	vdWs	Phe363-Lys381	vdWs
Phe151-Ser155	H-bond	Phe363-Ile382	vdWs
Phe151-Val216	vdWs	Phe363-Ile382	vdWs
Ser155-Pro158	vdWs	Phe363-Leu383	H-bond
Ser155-Val238	vdWs	Lys381-Val430	H-bond
Ser155-Val238	vdWs	Lys381-Met431	vdWs
Pro158-Lys162	H-bond	Leu383-Val430	vdWs
Pro158-Lys162	vdWs	Val405-Val430	vdWs
Pro158-Met204	vdWs	Asp411-Glu415	vdWs
Pro158-Ser207	vdWs	Trp412-Glu415	H-bond
Pro191-Ser197	H-bond	Gly420-Gly424	H-bond
Pro191-Ser197	vdWs	Gly424-Arg428	H-bond
Ser197-Gly200	vdWs	Gly424-Arg428	vdWs
Ser197-Lys201	H-bond	Glu425-Arg428	H-bond
Ser197-Lys201	vdWs	Glu425-Arg428	vdWs
Gly200-Met204	vdWs	Ala426-Val430	H-bond
Val218-Val247	H-bond	Ile427-Val430	H-bond
Lys226-Glu230	H-bond	Ile427-Met431	H-bond
Lys226-Glu230	vdWs	Ile427-Met431	vdWs
Leu227-Glu230	H-bond	Arg428-Asn432	H-bond
Leu227-Ala231	H-bond	Val430-Asp433	H-bond
Glu230-Gly234	H-bond	Val430-Leu436	vdWs
Glu230-Gly234	vdWs	Glu434-Val437	H-bond
Ala231-Gly234	vdWs	Asp446-Ala450	H-bond
Ala231-Lys236	H-bond	Asp446-Ala450	vdWs
Ala231-Lys236	vdWs	Ala447-Ala450	H-bond
Val238-Leu241	vdWs	Ala450-Cys457	H-bond
Val238-Leu241	vdWs	Gly456-Ala460	H-bond
Val247-Phe250	vdWs	Gly456-Ala460	vdWs
Val247-Phe250	vdWs	Cys457-Leu461	H-bond
Val247-Cys457	vdWs	Ala460-Leu464	H-bond

Node-Node	Interaction	Node-Node	Interaction
Tyr279-Phe363	π-π stacking	Ala460-Leu464	vdWs
Glu295-Gly420	vdWs	Leu461-Leu464	H-bond
Gly299-Ser303	H-bond	Leu461-Met465	H-bond
Gly299-Ser303	vdWs	Leu461-Met465	vdWs

Table S12 Interaction analysis of Mut10 based on second-level network.

Node-Node	Interaction	Node-Node	Interaction
Phe144-Phe151	π-π stacking	Asp298-Gly420	vdWs
Ser147-Phe151	H-bond	Gly299-Ser303	H-bond
Ala148-Phe151	vdWs	Leu300-Ser303	vdWs
Phe151-Phe154	π-π stacking	Lys302-Arg428	H-bond
Phe151-Phe154	H-bond	Lys302-Arg428	vdWs
Phe151-Ala155	H-bond	Ser303-Ala424	vdWs
Phe151-Leu232	vdWs	Ser303-Ala424	vdWs
Phe153-Phe157	π-π stacking	Ser303-Arg428	vdWs
Phe153-Phe157	H-bond	Trp305-Arg428	vdWs
Phe153-Phe157	vdWs	Trp305-Met431	vdWs
Phe154-Phe157	H-bond	Phe363-Ser371	vdWs
Phe157-Leu160	H-bond	Phe363-Ser371	vdWs
Phe157-Leu160	vdWs	Phe363-Ala375	vdWs
Phe157-Ala161	H-bond	Phe363-Pro381	H-bond
Phe157-Phe166	π-π stacking	Phe363-Ile382	vdWs
Phe157-Tyr200	π-π stacking	Phe363-Leu383	H-bond
Phe157-Phe203	π-π stacking	Pro381-Arg437	vdWs
Phe157-Phe203	vdWs	Gly420-Ala424	H-bond
Phe157-Phe203	vdWs	Glu421-Arg428	H-bond
Phe166-Leu193	vdWs	Ile423-Ile427	H-bond
Phe166-Tyr200	π-π stacking	Ala424-Ile427	vdWs
Pro191-Asp194	H-bond	Ala424-Arg428	H-bond
Pro191-Asp194	vdWs	Glu425-Arg428	H-bond
Pro191-Ser197	H-bond	Ile427-Met431	H-bond
Pro191-Phe199	vdWs	Ile427-Met431	vdWs
Pro191-Phe199	vdWs	Arg428-Asn432	H-bond
Asp194-Ser197	H-bond	Arg428-Asn432	vdWs
Asp194-Ser197	vdWs	Met431-Arg437	H-bond
Asp194-Tyr200	vdWs	Glu434-Arg437	vdWs
Pro195-Tyr200	vdWs	Glu434-Arg437	vdWs
Pro195-Tyr200	vdWs	Glu434-Met438	H-bond
Ser197-Tyr200	vdWs	Ser186-Lys392	H-bond
Ser197-Lys201	H-bond	Pro386-Lys392	vdWs
Ser197-Lys201	vdWs	Pro386-Lys392	vdWs
Tyr200-Met204	H-bond	Lys392-Glu396	H-bond
Tyr200-Met204	vdWs	Lys392-Glu396	vdWs
Met204-Pro208	vdWs	Lys392-Gly411	vdWs
Thr149-Ser179	vdWs	Lys392-Trp412	π-cation

Node-Node	Interaction	Node-Node	Interaction
Gly177-Glu227	vdWs	Lys392-Trp412	vdWs
Gly177-Ala231	vdWs	Val218-Val247	H-bond
Ser179-Glu227	vdWs	Val218-Val247	vdWs
Ser179-Ser228	H-bond	Val247-Phe250	vdWs
Ser179-Ser228	H-bond	Val247-Gln457	H-bond
Ser179-Ser228	vdWs	Pro249-Ala450	vdWs
Ser179-Ser228	vdWs	Asp446-Ala450	H-bond
Glu227-Ala231	H-bond	Ala447-Ala450	H-bond
Ser228-Ala231	vdWs	Ala450-Gln457	H-bond
Ala231-Lys236	H-bond	Ser456-Ala460	H-bond
Ala231-Lys236	vdWs	Gln457-Ala460	vdWs
Ala231-Lys236	vdWs	Gln457-Leu461	H-bond
Ala231-Val237	vdWs	Gln457-Leu461	vdWs
Gly275-Lys358	H-bond	Ala460-Leu464	H-bond
Gly275-Ala359	vdWs	Ala460-Leu464	vdWs
Gly275-Arg437	H-bond	Leu461-Leu464	H-bond
Tyr279-Phe363	π-π stacking	Leu461-Met465	H-bond
Glu295-Gly420	H-bond		

Table S13 The number of interactions between different edge types of WT and Mut10 based on second-level network.

Interaction	WT	Mut10
H-bond	34	44
π-π stacking	3	8
π-cation	0	1
Ionic bond	0	0
π-H bond	0	0
vdWs	47	58
Total number	84	111

Table S14 Interaction analysis of WT based on overall network.

Node-Node	Interaction	Node-Node	Interaction
His16-His44	π-π stacking	Leu232-Val237	vdWs
His16-His44	π-H bond	Leu232-Val244	vdWs
His16-Thr46	H-bond	Asn233-Val244	H-bond
His16-Leu112	vdWs	Asn233-Val244	H-bond
His16-Pro114	H-bond	Val238-Leu241	vdWs
His16-Ser117	H-bond	Val238-Leu241	vdWs
Val17-His44	H-bond	Val247-Phe250	vdWs
Val17-His44	vdWs	Val247-Phe250	vdWs
Val17-Val45	vdWs	Val247-Cys457	vdWs
Ala18-Ser118	H-bond	Pro249-Ile451	vdWs
Ala18-Ile120	H-bond	Val251-Trp377	vdWs
Leu19-Thr46	H-bond	Cys253-Glu256	H-bond
Leu19-Ile48	H-bond	Cys253-Glu256	vdWs
Leu19-Ile120	vdWs	Glu254-Lys257	H-bond
Leu20-Ile48	vdWs	Glu254-Lys257	vdWs
Leu20-Ile120	H-bond	Lys257-Glu353	vdWs
Leu20-Tyr121	vdWs	Lys260-Glu263	vdWs
Leu20-Asp122	vdWs	Ile265-Trp268	H-bond
Ser22-Asp122	vdWs	Ile265-Leu269	H-bond
Ser22-Asp122	vdWs	Ile265-Val345	vdWs
Ala23-Val54	vdWs	Ser266-Leu269	vdWs
Ala23-Gln94	vdWs	Ser266-Asp270	vdWs
Gly24-His27	H-bond	Glu267-Asp270	vdWs
Gly24-His27	vdWs	Trp268-Glu271	vdWs
Gly24-Leu28	H-bond	Trp268-Gln272	H-bond
Gly24-Leu28	vdWs	Trp268-Gln272	vdWs
Gly24-Glu58	H-bond	Trp268-Lys341	vdWs
Met25-Thr29	vdWs	Trp268-Lys341	vdWs
Gly26-Asn370	H-bond	Trp268-Leu343	vdWs
His27-Phe31	vdWs	Leu269-Leu308	vdWs
His27-Asp122	Ionic bond	Leu269-Leu308	vdWs
His27-Asp122	H-bond	Leu269-His357	vdWs
Leu28-Leu32	H-bond	Leu269-His357	vdWs
Leu28-Leu32	vdWs	Asp270-His357	H-bond
Thr29-Arg33	H-bond	Pro273-Ser276	vdWs
Thr29-Arg33	vdWs	Pro273-Arg306	vdWs
Pro30-Leu34	H-bond	Ser274-Lys358	vdWs
Phe31-Leu34	H-bond	Ser274-Lys358	vdWs

Node-Node	Interaction	Node-Node	Interaction
Phe31-Ala35	H-bond	Gly275-Lys358	H-bond
Phe31-Tyr121	vdWs	Ser276-Trp305	vdWs
Phe31-Asp122	vdWs	Ser276-Arg306	vdWs
Leu32-Ala35	H-bond	Ser276-Arg306	vdWs
Leu32-Ser36	H-bond	Ser276-Ala359	H-bond
Leu32-Leu61	vdWs	Val277-Ala359	H-bond
Leu32-Phe65	vdWs	Val277-Gly361	H-bond
Arg33-Leu37	H-bond	Val278-Arg306	H-bond
Arg33-Phe250	vdWs	Val278-Phe307	vdWs
Arg33-Glu256	Ionic bond	Val278-Leu308	H-bond
Arg33-Glu256	H-bond	Val278-Val364	vdWs
Arg33-Glu256	H-bond	Tyr279-Phe363	π-π stacking
Arg33-Glu256	vdWs	Tyr279-Val364	H-bond
Arg33-Glu374	H-bond	Tyr279-Val364	vdWs
Arg33-Glu374	H-bond	Val280-Leu300	vdWs
Leu34-Leu37	vdWs	Val280-Leu308	H-bond
Leu34-Leu38	H-bond	Val280-Val310	H-bond
Leu34-Leu38	vdWs	Val280-Val364	vdWs
Leu34-Phe250	vdWs	Ser281-Val364	H-bond
Ala35-Leu38	H-bond	Phe282-Trp309	π-π stacking
Ala35-Leu39	H-bond	Phe282-His366	vdWs
Ser36-Leu39	vdWs	Phe282-Trp385	π-π stacking
Ser36-His40	H-bond	Phe282-Trp385	vdWs
Ser36-His40	vdWs	Phe282-Leu387	vdWs
Leu37-Cys457	vdWs	Gly283-His366	π-H bond
Leu38-Gln41	H-bond	Thr286-Lys312	vdWs
Leu39-His42	H-bond	Ala287-Glu413	H-bond
Gln41-Gln462	H-bond	Met288-Leu293	vdWs
Val45-Asn73	H-bond	Met288-Leu293	vdWs
Thr46-Asn73	vdWs	Gly289-Gln292	vdWs
Thr46-Asn73	vdWs	Gly289-Leu293	H-bond
Thr46-Leu112	vdWs	Glu291-Arg294	H-bond
Leu47-Asn73	H-bond	Gln292-Glu295	vdWs
Leu47-Gln74	vdWs	Gln292-Val296	vdWs
Leu47-Leu75	H-bond	Gln292-Val418	H-bond
Leu47-Leu75	vdWs	Gln292-Val418	H-bond
Ile48-Leu75	vdWs	Gln292-Val418	vdWs
Ile48-Leu109	vdWs	Leu293-Val296	vdWs
Thr49-Leu75	vdWs	Arg294-Asp298	H-bond

Node-Node	Interaction	Node-Node	Interaction
Thr49-Phe77	H-bond	Arg294-Asp298	vdWs
Gln51-His76	vdWs	Arg294-Val327	vdWs
Gln51-Phe77	H-bond	Glu295-Asp298	H-bond
Val54-Phe91	vdWs	Glu295-Gly299	H-bond
Ser55-Glu58	H-bond	Glu295-Gly299	vdWs
Ser55-Glu58	vdWs	Glu295-Val418	vdWs
Ser55-Glu58	vdWs	Glu295-Gly420	vdWs
Ser55-Phe91	vdWs	Glu295-Ile423	vdWs
Lys56-Glu59	H-bond	Val296-Gly299	H-bond
Lys56-Asp60	H-bond	Val296-Gly299	vdWs
Ala57-Asp60	H-bond	Val296-Leu300	H-bond
Ala57-Leu61	H-bond	Asp298-Val301	vdWs
Glu58-Leu62	H-bond	Asp298-Lys302	Ionic bond
Glu59-Ser63	H-bond	Asp298-Lys302	H-bond
Asp60-Arg64	H-bond	Gly299-Lys302	vdWs
Leu61-Arg64	vdWs	Gly299-Ser303	H-bond
Leu61-Phe65	H-bond	Gly299-Ser303	vdWs
Leu61-Phe65	vdWs	Gly299-Gly420	vdWs
Leu62-Phe65	H-bond	Leu300-Ser303	vdWs
Leu62-Phe65	vdWs	Val301-Gly304	vdWs
Leu62-Leu66	H-bond	Val301-Arg335	vdWs
Leu62-Leu66	vdWs	Lys302-Arg428	H-bond
Leu62-Leu66	vdWs	Ser303-Gly424	vdWs
Ser63-Ser67	H-bond	Gly304-Lys341	H-bond
Ser63-Ser67	vdWs	Phe307-Met336	vdWs
Arg64-Ala68	H-bond	Phe307-Lys341	H-bond
Arg64-Phe255	H-bond	Phe307-Leu343	H-bond
Arg64-Glu256	vdWs	Leu308-Ile354	vdWs
Phe65-Ala68	vdWs	Trp309-Leu343	H-bond
Phe65-Phe69	π-π stacking	Trp309-Val345	H-bond
Phe65-Phe69	H-bond	Val310-Val345	vdWs
Phe65-Phe69	vdWs	Val311-Val345	H-bond
Phe65-Phe255	π-π stacking	Val311-Val345	vdWs
Phe65-Phe255	vdWs	Gly329-Leu332	H-bond
Leu66-Phe69	vdWs	Gly329-Val333	H-bond
Leu66-Gln74	vdWs	Gly329-Val333	vdWs
Phe69-Val72	vdWs	Phe330-Glu334	H-bond
Phe69-Phe255	π-π stacking	Glu331-Arg335	H-bond
Asn73-Leu112	vdWs	Glu331-Arg335	vdWs

Node-Node	Interaction	Node-Node	Interaction
Phe77-Ser101	vdWs	Leu332-Arg335	vdWs
Phe77-Ser102	vdWs	Leu332-Met336	H-bond
Phe77-Ser102	vdWs	Val333-Val337	H-bond
Phe77-Leu105	vdWs	Val333-Val337	vdWs
Phe77-Leu105	vdWs	Glu334-Val337	H-bond
Pro80-Ser101	vdWs	Glu334-Lys338	H-bond
Pro90-Leu93	H-bond	Arg335-Glu339	Ionic bond
Gln94-Ile98	H-bond	Arg335-Glu339	H-bond
Phe95-Arg99	vdWs	Arg335-Glu339	H-bond
Ala96-Arg99	H-bond	Arg335-Glu339	H-bond
Ala96-Arg99	vdWs	Arg335-Glu339	vdWs
Ala96-Ser100	H-bond	Arg335-Glu339	vdWs
Ile98-Ser101	vdWs	Val337-Lys340	vdWs
Ile98-Ser102	H-bond	Val345-Val349	vdWs
Ser101-Leu104	H-bond	Asp350-Glu353	H-bond
Ser101-Leu104	vdWs	Asp350-Glu353	vdWs
Ser102-Leu105	H-bond	Asp350-Ile354	H-bond
Leu105-Leu109	H-bond	Gln351-Ile354	vdWs
Thr106-Ser110	H-bond	Gln351-Leu355	H-bond
Thr106-Ser110	vdWs	Gln351-Ser371	H-bond
Pro107-Ser111	H-bond	Gln351-Glu374	H-bond
Pro107-Ser111	vdWs	Ser352-Gly356	H-bond
Leu116-Val138	vdWs	Glu353-Gly356	vdWs
Ser118-Pro139	vdWs	Glu353-His357	H-bond
Ser118-Trp468	π-H bond	Ile354-His357	H-bond
Ser118-Trp468	vdWs	Ile354-Val360	vdWs
Phe119-Pro139	H-bond	His357-Val360	H-bond
Phe119-His140	vdWs	Gly362-Met431	vdWs
Tyr121-Leu143	H-bond	Phe363-Ser371	vdWs
Asp122-Leu125	H-bond	Phe363-Val380	vdWs
Asp122-Leu125	vdWs	Phe363-Lys381	vdWs
Met123-Ile126	H-bond	Phe363-Ile382	vdWs
Met123-Ile126	vdWs	Phe363-Ile382	vdWs
Met123-Phe144	vdWs	Phe363-Leu383	H-bond
Leu125-Pro128	vdWs	Val364-Leu383	vdWs
Leu125-Leu129	H-bond	Ser365-Leu383	H-bond
Ile126-Leu130	vdWs	Ser365-Trp385	H-bond
Ile126-Asp206	vdWs	His366-Trp385	vdWs
Ile126-Leu213	vdWs	Cys367-Gly384	vdWs

Node-Node	Interaction	Node-Node	Interaction
Pro128-Pro131	vdWs	Cys367-Asn394	H-bond
Leu129-Ile132	vdWs	Gly368-Ser371	H-bond
Leu129-Ala133	H-bond	Gly368-Ser371	vdWs
Leu129-Ala133	vdWs	Gly368-Val372	H-bond
Leu130-Ala133	H-bond	Trp369-Val372	vdWs
Leu130-Glu134	H-bond	Trp369-Val373	H-bond
Pro131-Ser135	H-bond	Trp369-Val373	vdWs
Ile132-Leu136	vdWs	Asn370-Glu374	H-bond
Ala133-Leu136	H-bond	Ser371-Ala375	H-bond
His140-Lys212	H-bond	Val372-Ala376	H-bond
His140-His214	π-π stacking	Val373-Ala376	vdWs
His140-His214	H-bond	Val373-Trp377	H-bond
His140-His214	vdWs	Glu374-Trp377	H-bond
Tyr141-His214	π-π stacking	Glu374-Trp377	vdWs
Tyr141-Tyr245	π-π stacking	Glu374-Phe378	H-bond
Tyr141-Trp468	π-π stacking	Ala375-Val380	H-bond
Tyr141-Trp468	H-bond	Ala375-Val380	vdWs
Tyr141-Trp468	vdWs	Ala376-Trp403	vdWs
Ile142-Gly215	vdWs	Trp377-Lys444	vdWs
Ile142-Leu217	H-bond	Trp377-Arg448	vdWs
Phe144-Met150	vdWs	Lys381-Val430	H-bond
Phe144-Phe151	π-π stacking	Lys381-Met431	vdWs
Phe144-Leu217	H-bond	Ile382-Trp403	H-bond
Ser146-Asp390	H-bond	Ile382-Val405	H-bond
Ser146-Asn394	H-bond	Ile382-Val405	vdWs
Ser147-Met150	H-bond	Leu383-Ala426	vdWs
Ser147-Met150	vdWs	Leu383-Val430	vdWs
Ser147-Met150	vdWs	Gly384-Val405	H-bond
Ser147-Phe151	H-bond	Trp385-Trp410	π-π stacking
Ser147-Asn394	H-bond	Trp385-Trp410	π-π stacking
Ala148-Phe151	vdWs	Trp385-Trp410	vdWs
Ala148-Ser152	H-bond	Pro386-Gln391	vdWs
Ala148-Val218	vdWs	Pro386-Lys392	vdWs
Ala148-Glu225	H-bond	Leu387-Gln391	H-bond
Ala148-Glu225	vdWs	Leu387-Gln391	vdWs
Ala148-Glu225	vdWs	Leu387-Glu413	H-bond
Thr149-Ser152	H-bond	Leu387-Glu413	vdWs
Thr149-Phe153	H-bond	His388-Gln391	H-bond
Thr149-Phe153	vdWs	His388-Gln391	H-bond

Node-Node	Interaction	Node-Node	Interaction
Thr149-Glu225	vdWs	His388-Gln391	vdWs
Met150-Phe153	H-bond	His388-Gln391	vdWs
Met150-Phe153	vdWs	His388-Trp412	vdWs
Met150-Phe154	H-bond	His388-Glu413	Ionic bond
Met150-Asp390	vdWs	His388-Glu413	H-bond
Phe151-Phe154	π-π stacking	His388-Glu413	vdWs
Phe151-Phe154	vdWs	Asp390-Asn394	H-bond
Phe151-Ser155	H-bond	Gln391-Ala395	H-bond
Phe151-Val216	vdWs	Gln391-Ala395	vdWs
Ser152-Tyr156	vdWs	Lys392-Glu396	H-bond
Ser152-Leu232	vdWs	Lys392-Trp412	π-cation
Phe153-Phe157	H-bond	Ile393-Glu396	H-bond
Phe153-Ile183	vdWs	Ile393-Val397	H-bond
Phe154-Phe157	vdWs	Ile393-Val397	vdWs
Phe154-Phe203	π-π stacking	Asn394-Val397	vdWs
Phe154-Phe203	vdWs	Asn394-Val398	H-bond
Phe154-Asp206	vdWs	Ala395-Val398	vdWs
Phe154-Ser207	H-bond	Ala395-Ala399	H-bond
Phe154-Ser207	vdWs	Glu396-Ala399	vdWs
Ser155-Pro158	vdWs	Glu396-Lys400	H-bond
Ser155-Val238	vdWs	Glu396-Lys400	vdWs
Ser155-Val238	vdWs	Glu396-Trp406	H-bond
Tyr156-Leu160	H-bond	Val398-Gly401	H-bond
Phe157-Leu160	H-bond	Ala399-Gly402	H-bond
Phe157-Leu160	vdWs	Gly402-Leu436	vdWs
Phe157-Ala161	H-bond	Gly402-Lys439	vdWs
Phe157-Phe166	π-π stacking	Val405-Val430	vdWs
Phe157-Phe203	π-π stacking	Lys407-Glu429	Ionic bond
Pro158-Lys162	H-bond	Lys407-Glu429	H-bond
Pro158-Lys162	vdWs	Gly409-Arg416	H-bond
Pro158-Met204	vdWs	Asp411-Glu415	vdWs
Pro158-Ser207	vdWs	Trp412-Glu415	H-bond
Leu160-Leu170	vdWs	Arg416-Glu422	Ionic bond
Ala161-Phe166	vdWs	Arg416-Glu422	H-bond
Pro167-Arg185	H-bond	Arg416-Glu422	H-bond
Pro167-Arg185	vdWs	Arg416-Glu422	vdWs
Asp171-Arg185	H-bond	Val418-Ile423	vdWs
Val173-Ile183	H-bond	Lys419-Glu422	H-bond
Val173-Ile183	H-bond	Lys419-Glu422	H-bond

Node-Node	Interaction	Node-Node	Interaction
Val173-Ile183	vdWs	Lys419-Ile423	H-bond
Ile175-Val178	vdWs	Gly420-Gly424	H-bond
Ile175-Val237	vdWs	Glu421-Glu425	H-bond
Pro176-Lys236	vdWs	Glu421-Glu425	vdWs
Val178-Ser228	vdWs	Glu422-Glu425	vdWs
Ser179-Ser228	H-bond	Glu422-Ala426	H-bond
Val180-Ile183	vdWs	Ile423-Ala426	vdWs
Pro184-Ser187	H-bond	Ile423-Ile427	H-bond
Arg185-Ile188	H-bond	Gly424-Arg428	H-bond
Ser186-Lys392	H-bond	Gly424-Arg428	vdWs
Ser186-Lys392	vdWs	Glu425-Arg428	H-bond
Ser187-Trp412	vdWs	Glu425-Arg428	vdWs
Ile188-Leu193	vdWs	Glu425-Glu429	H-bond
Pro189-Leu192	H-bond	Ala426-Glu429	H-bond
Pro189-Leu192	vdWs	Ala426-Val430	H-bond
Pro190-Leu193	H-bond	Ile427-Val430	H-bond
Pro190-Leu193	vdWs	Ile427-Met431	H-bond
Pro191-Ser197	H-bond	Ile427-Met431	vdWs
Pro191-Ser197	vdWs	Arg428-Asn432	H-bond
Ser197-Gly200	vdWs	Glu429-Asp433	vdWs
Ser197-Lys201	H-bond	Val430-Asp433	H-bond
Ser197-Lys201	vdWs	Val430-Leu436	vdWs
Leu198-Lys201	H-bond	Asp433-Leu436	vdWs
Leu198-Leu202	H-bond	Asp433-Leu436	vdWs
Leu198-Leu202	vdWs	Glu434-Val437	H-bond
Phe199-Leu202	vdWs	Ser435-Met438	vdWs
Phe199-Phe203	π-π stacking	Ser435-Lys439	H-bond
Phe199-Phe203	H-bond	Leu436-Ala440	H-bond
Phe199-Phe203	vdWs	Leu436-Ala440	vdWs
Gly200-Met204	vdWs	Met438-Gln442	H-bond
Leu202-Glu205	H-bond	Lys439-Val443	H-bond
Leu202-Asp206	H-bond	Ala440-Lys444	H-bond
Leu202-Asp206	vdWs	Ala440-Lys444	vdWs
Phe203-Ser207	H-bond	Thr441-Lys444	H-bond
Glu205-Pro208	vdWs	Thr441-Lys445	H-bond
Glu205-Lys209	H-bond	Thr441-Lys445	vdWs
Glu205-Lys209	vdWs	Gln442-Lys445	H-bond
Asp206-Lys209	H-bond	Gln442-Lys445	vdWs
Asp206-Lys209	vdWs	Gln442-Asp446	H-bond

Node-Node	Interaction	Node-Node	Interaction
Ser207-Leu210	H-bond	Gln442-Asp446	vdWs
Ser207-Leu210	vdWs	Val443-Asp446	H-bond
Lys209-Lys212	H-bond	Val443-Asp446	vdWs
Lys209-Leu213	vdWs	Val443-Ala447	H-bond
Leu210-Leu213	vdWs	Lys444-Ala447	vdWs
Leu210-Pro242	vdWs	Lys444-Arg448	H-bond
Leu213-Pro242	vdWs	Lys445-Arg448	vdWs
Val216-Pro243	H-bond	Lys445-Lys449	H-bond
Val218-Tyr245	H-bond	Asp446-Ala450	H-bond
Val218-Val247	H-bond	Asp446-Ala450	vdWs
Asn219-Pro249	vdWs	Ala447-Ala450	H-bond
Asn219-Phe250	H-bond	Arg448-Ile451	vdWs
Asn219-Trp369	H-bond	Lys449-Gly455	H-bond
Asn219-Val373	vdWs	Ala450-Cys457	H-bond
Thr220-Glu225	vdWs	Gly455-Glu458	H-bond
Thr220-Gly248	H-bond	Gly455-Val459	H-bond
Thr220-Gly248	vdWs	Gly455-Val459	vdWs
Thr220-Trp369	vdWs	Gly455-Val459	vdWs
Phe221-Ile224	H-bond	Gly456-Ala460	H-bond
Phe221-Glu225	H-bond	Gly456-Ala460	vdWs
Phe221-Pro249	vdWs	Cys457-Leu461	H-bond
Phe221-Ala447	vdWs	Glu458-Gln462	H-bond
Glu222-Lys226	H-bond	Val459-Gln462	H-bond
Glu222-Lys226	vdWs	Val459-Lys463	H-bond
Ile224-Trp369	vdWs	Ala460-Leu464	H-bond
Lys226-Glu230	H-bond	Ala460-Leu464	vdWs
Lys226-Glu230	vdWs	Leu461-Leu464	H-bond
Leu227-Glu230	H-bond	Leu461-Met465	H-bond
Leu227-Ala231	H-bond	Leu461-Met465	vdWs
Ser228-Leu232	H-bond	Gln462-Glu466	vdWs
Leu229-Asn233	H-bond	Lys463-Glu466	vdWs
Leu229-Asn233	vdWs	Lys463-Glu466	vdWs
Glu230-Gly234	H-bond	Leu464-Val467	vdWs
Glu230-Gly234	vdWs	Leu464-Trp468	H-bond
Ala231-Gly234	vdWs	Leu464-Trp468	vdWs
Ala231-Lys236	H-bond	Leu464-Trp468	vdWs
Ala231-Lys236	vdWs		

Table S15 Interaction analysis of Mut10 based on overall network.

Node-Node	Interaction	Node-Node	Interaction
His16-His44	π-π stacking	Ser228-Ala231	vdWs
His16-His44	π-H bond	Ser228-Leu232	H-bond
His16-His44	vdWs	Leu229-Asn233	H-bond
His16-His44	vdWs	Glu230-Asn233	H-bond
His16-Thr46	H-bond	Glu230-Gly234	H-bond
His16-Thr46	vdWs	Glu230-Lys236	vdWs
His16-Pro114	H-bond	Ala231-Lys236	H-bond
His16-Ser117	H-bond	Ala231-Lys236	vdWs
His16-Ser117	H-bond	Ala231-Lys236	vdWs
His16-Ser117	vdWs	Ala231-Val237	vdWs
His16-Ser117	vdWs	Leu232-Val244	vdWs
His16-Ser118	H-bond	Asn233-Val244	H-bond
Val17-His44	H-bond	Asn233-Val244	H-bond
Ala18-Leu116	vdWs	Asn233-Val244	vdWs
Ala18-Ser118	H-bond	Val238-Leu241	vdWs
Ala18-Ser118	vdWs	Val247-Phe250	vdWs
Ala18-Phe119	vdWs	Val247-Gln457	H-bond
Ala18-Ile120	H-bond	Pro249-Ala450	vdWs
Leu19-Thr46	H-bond	Pro252-Glu256	vdWs
Leu19-Ile48	H-bond	Pro252-Ser352	vdWs
Leu20-Ile48	vdWs	Cys253-Glu256	H-bond
Leu20-Leu105	vdWs	Cys253-Glu256	H-bond
Leu20-Ile120	H-bond	Cys253-Glu256	vdWs
Leu20-Ile120	vdWs	Glu254-Lys257	H-bond
Leu20-Asp122	H-bond	Glu254-Lys257	vdWs
Ser22-Asp122	H-bond	Arg261-Trp348	H-bond
Ser22-Asp122	vdWs	Arg261-Trp348	H-bond
Ser22-Asp122	vdWs	Arg261-Asp350	vdWs
Ser22-Thr124	H-bond	Glu263-Ser266	H-bond
Ala23-Gln94	vdWs	Glu263-Glu267	H-bond
Ala23-Gln94	vdWs	Thr264-Glu267	vdWs
Gly24-His27	H-bond	Thr264-Trp268	H-bond
Gly24-His27	vdWs	Ile265-Trp268	H-bond
Gly24-Leu28	H-bond	Ile265-Leu269	H-bond
Gly24-Glu58	H-bond	Ser266-Leu269	vdWs
Gly24-Phe91	vdWs	Ser266-Asp270	H-bond
Met25-Leu61	vdWs	Glu267-Asp270	vdWs
Gly26-Asn370	H-bond	Glu267-Asp270	vdWs

Node-Node	Interaction	Node-Node	Interaction
Gly26-Asn370	vdWs	Trp268-Glu271	H-bond
His27-Phe31	vdWs	Trp268-Gln272	H-bond
His27-Asp122	Ionic bond	Leu269-Gln272	H-bond
His27-Asp122	H-bond	Leu269-His357	vdWs
Leu28-Phe31	H-bond	Asp270-His357	H-bond
Leu28-Phe31	vdWs	Gln272-Arg306	H-bond
Leu28-Leu32	H-bond	Gln272-Arg306	vdWs
Leu28-Leu62	vdWs	Pro273-Ser276	vdWs
Thr29-Arg33	H-bond	Pro273-Ala359	vdWs
Pro30-Leu34	H-bond	Ser274-Lys358	vdWs
Phe31-Ala35	H-bond	Ser274-Lys358	vdWs
Phe31-Asp122	vdWs	Gly275-Lys358	H-bond
Phe31-Leu143	vdWs	Gly275-Ala359	vdWs
Leu32-Ala35	vdWs	Gly275-Arg437	H-bond
Leu32-Ser36	H-bond	Ser276-Arg306	H-bond
Leu32-Leu61	vdWs	Ser276-Ala359	H-bond
Arg33-Leu37	H-bond	Ser276-Ala359	vdWs
Arg33-Phe250	vdWs	Val277-Arg306	vdWs
Arg33-Glu256	Ionic bond	Val277-Ala359	H-bond
Arg33-Glu256	H-bond	Val277-Gly361	H-bond
Arg33-Glu256	H-bond	Val278-Arg306	H-bond
Arg33-Glu256	vdWs	Val278-Phe307	vdWs
Arg33-Glu374	H-bond	Val278-Leu308	H-bond
Arg33-Glu374	H-bond	Val278-Gly362	vdWs
Arg33-Glu374	vdWs	Val278-Val364	vdWs
Leu34-Leu37	H-bond	Tyr279-Phe363	π-π stacking
Leu34-Leu37	vdWs	Tyr279-Val364	H-bond
Leu34-Leu38	H-bond	Val280-Leu308	H-bond
Ala35-Leu38	H-bond	Val280-Val310	H-bond
Ala35-Leu39	H-bond	Val280-Val364	vdWs
Ala35-Leu39	vdWs	Ser281-Val364	H-bond
Ser36-Leu39	vdWs	Ser281-Val364	vdWs
Ser36-His40	H-bond	Phe282-Trp309	π-π stacking
Leu37-His40	vdWs	Phe282-Trp385	π-π stacking
Leu37-Gln41	H-bond	Gly283-His366	π-H bond
Leu37-Gln41	vdWs	Gly283-His366	vdWs
Leu38-Gln41	vdWs	Ser284-Lys312	vdWs
Leu38-Cys43	H-bond	Ser284-Trp348	vdWs
Leu39-His42	H-bond	Thr286-Asp313	vdWs

Node-Node	Interaction	Node-Node	Interaction
Cys43-Met465	vdWs	Ala287-His388	H-bond
Val45-Val72	vdWs	Ala287-His388	vdWs
Val45-Asn73	H-bond	Ala287-His388	vdWs
Thr46-Asn73	H-bond	Ala287-Glu413	vdWs
Thr46-Asn73	vdWs	Met288-Gln292	vdWs
Leu47-Asn73	H-bond	Gly289-Leu293	H-bond
Leu47-Leu75	H-bond	Gly289-Glu413	H-bond
Ile48-Leu75	vdWs	Arg290-Leu293	H-bond
Ile48-Leu109	vdWs	Arg290-Leu293	vdWs
Thr49-Gln74	H-bond	Arg290-Arg294	H-bond
Thr49-Phe77	H-bond	Gln292-Glu295	vdWs
Pro50-Leu79	vdWs	Gln292-Val296	H-bond
Gln51-His76	vdWs	Gln292-Val296	vdWs
Gln51-Phe77	H-bond	Gln292-Val418	H-bond
Gln51-Leu79	H-bond	Gln292-Val418	H-bond
Gln51-Leu79	vdWs	Gln292-Val418	vdWs
Val54-Glu58	vdWs	Leu293-Val296	H-bond
Val54-Phe91	vdWs	Leu293-Gly297	H-bond
Ser55-Glu58	H-bond	Leu293-Leu328	vdWs
Ser55-Glu58	H-bond	Arg294-Gly297	H-bond
Ser55-Glu59	H-bond	Arg294-Asp298	H-bond
Lys56-Glu59	H-bond	Arg294-Leu328	vdWs
Lys56-Asp60	H-bond	Glu295-Asp298	H-bond
Lys56-Asp60	H-bond	Glu295-Asp298	vdWs
Lys56-Asp317	H-bond	Glu295-Gly299	H-bond
Lys56-Asp317	vdWs	Glu295-Val418	vdWs
Ala57-Asp60	vdWs	Glu295-Lys419	vdWs
Ala57-Leu61	H-bond	Glu295-Gly420	H-bond
Glu58-Leu62	H-bond	Val296-Gly299	H-bond
Glu58-Leu62	vdWs	Val296-Gly299	vdWs
Glu59-Leu62	vdWs	Val296-Leu300	H-bond
Glu59-Ser63	H-bond	Val296-Trp385	vdWs
Glu59-Ser63	vdWs	Gly297-Leu300	vdWs
Asp60-Arg64	H-bond	Gly297-Val301	H-bond
Leu61-Arg64	vdWs	Asp298-Val301	vdWs
Leu61-Phe65	H-bond	Asp298-Lys302	Ionic bond
Leu62-Phe65	H-bond	Asp298-Lys302	H-bond
Leu62-Phe65	vdWs	Asp298-Lys302	H-bond
Leu62-Leu66	H-bond	Asp298-Lys302	vdWs

Node-Node	Interaction	Node-Node	Interaction
Ser63-Ser67	H-bond	Asp298-Lys302	vdWs
Arg64-Ala68	H-bond	Asp298-Leu332	vdWs
Arg64-Phe255	H-bond	Asp298-Gly420	vdWs
Arg64-Glu256	H-bond	Gly299-Ser303	H-bond
Arg64-Val258	vdWs	Gly299-Ile423	vdWs
Phe65-Ala68	H-bond	Leu300-Ser303	vdWs
Phe65-Ala68	vdWs	Leu300-Phe307	vdWs
Phe65-Phe69	π-π stacking	Val301-Gly304	H-bond
Phe65-Phe69	H-bond	Val301-Arg335	vdWs
Phe65-Phe255	π-π stacking	Val301-Met336	vdWs
Phe65-Phe255	vdWs	Lys302-Arg428	H-bond
Leu66-Phe69	vdWs	Lys302-Arg428	vdWs
Leu66-Pro70	vdWs	Ser303-Ala424	vdWs
Leu66-Gln74	vdWs	Ser303-Ala424	vdWs
Phe69-Val72	H-bond	Ser303-Arg428	vdWs
Phe69-Val72	vdWs	Gly304-Lys341	vdWs
Phe69-Phe255	π-π stacking	Trp305-Arg428	vdWs
Leu75-Leu108	vdWs	Trp305-Met431	vdWs
Leu79-Gln94	vdWs	Phe307-Lys341	H-bond
Pro80-Ser101	vdWs	Phe307-Lys341	vdWs
Pro90-Gln94	H-bond	Phe307-Leu343	H-bond
Phe91-Gln94	vdWs	Leu308-Leu343	vdWs
Phe91-Phe95	H-bond	Trp309-Leu328	vdWs
Phe91-Arg285	π-cation	Trp309-Leu343	H-bond
Phe91-Arg285	vdWs	Trp309-Val344	vdWs
Phe92-Phe95	π-π stacking	Trp309-Val345	H-bond
Phe92-Phe95	vdWs	Trp309-Val345	vdWs
Phe92-Ala96	H-bond	Val310-Val345	vdWs
Phe92-Leu198	vdWs	Val311-Val345	H-bond
Leu93-Ser97	H-bond	Lys312-Trp348	vdWs
Gln94-Ser97	H-bond	Asp325-Gly329	H-bond
Gln94-Ile98	H-bond	Asp325-Phe330	vdWs
Phe95-Thr124	vdWs	Asp325-Val333	vdWs
Ser97-Ser100	H-bond	Gly329-Val333	H-bond
Ser97-Ser101	H-bond	Phe330-Val333	H-bond
Ile98-Ser101	vdWs	Phe330-Val333	vdWs
Ile98-Ser102	H-bond	Phe330-Glu334	H-bond
Arg99-Pro128	vdWs	Glu331-Glu334	vdWs
Ser101-Leu104	H-bond	Glu331-Arg335	H-bond

Node-Node	Interaction	Node-Node	Interaction
Ser102-Leu105	H-bond	Leu332-Met336	H-bond
Ser102-Leu105	vdWs	Leu332-Met336	vdWs
Leu104-Pro107	vdWs	Val333-Met336	H-bond
Leu105-Leu108	H-bond	Val333-Val337	H-bond
Leu105-Leu108	vdWs	Val333-Val337	vdWs
Leu105-Leu108	vdWs	Glu334-Val337	vdWs
Leu105-Leu109	H-bond	Glu334-Val337	vdWs
Leu105-Leu109	vdWs	Glu334-Lys338	H-bond
Thr106-Leu109	H-bond	Glu334-Lys338	vdWs
Thr106-Ser110	H-bond	Glu334-Lys338	vdWs
Pro107-Ser111	H-bond	Arg335-Lys338	vdWs
Leu109-Leu112	vdWs	Arg335-Glu339	H-bond
Ser110-Leu136	vdWs	Arg335-Glu339	H-bond
Ser118-Trp468	π-H bond	Arg335-Glu339	vdWs
Ser118-Trp468	vdWs	Met336-Lys340	H-bond
Phe119-Pro139	H-bond	Met336-Val344	vdWs
Tyr121-Leu130	vdWs	Asp350-Glu353	H-bond
Tyr121-His140	π-π stacking	Asp350-Glu353	H-bond
Tyr121-His140	H-bond	Asp350-Glu353	vdWs
Tyr121-His140	vdWs	Gln351-Ile354	H-bond
Tyr121-Tyr141	vdWs	Gln351-Leu355	H-bond
Tyr121-Leu143	H-bond	Gln351-Ser371	H-bond
Tyr121-Leu213	vdWs	Gln351-Glu374	H-bond
Asp122-Leu125	H-bond	Ser352-Gly356	H-bond
Met123-Ile126	vdWs	Glu353-His357	vdWs
Met123-Leu143	H-bond	Ile354-His357	H-bond
Met123-Phe144	vdWs	Ile354-His357	vdWs
Leu125-Pro128	vdWs	Ile354-Val360	vdWs
Leu125-Leu129	H-bond	Leu355-Phe378	vdWs
Leu125-Leu129	vdWs	His357-Val360	H-bond
Ile126-Leu130	H-bond	Phe363-Ser371	vdWs
Ile126-Asp206	vdWs	Phe363-Ser371	vdWs
Leu129-Ile132	vdWs	Phe363-Ala375	vdWs
Leu129-Ala133	H-bond	Phe363-Pro381	H-bond
Leu130-Glu134	H-bond	Phe363-Ile382	vdWs
Leu130-Lys209	vdWs	Phe363-Leu383	H-bond
Pro131-Ser135	H-bond	Ser365-Leu383	H-bond
Pro131-Ser135	vdWs	Ser365-Trp385	H-bond
Ile132-Ser135	H-bond	Ser365-Trp385	vdWs

Node-Node	Interaction	Node-Node	Interaction
Ala133-Leu136	H-bond	His366-Trp385	vdWs
Ala133-Leu136	vdWs	His366-Gln391	vdWs
Glu134-Gly137	vdWs	Cys367-Val372	vdWs
His140-Lys212	vdWs	Cys367-Asn394	H-bond
His140-Leu213	vdWs	Cys367-Ala395	vdWs
His140-Leu213	vdWs	Cys367-Ala395	vdWs
His140-His214	π-π stacking	Gly368-Ser371	H-bond
His140-His214	H-bond	Gly368-Ser371	vdWs
His140-His214	vdWs	Gly368-Val372	H-bond
His140-His214	vdWs	Gly368-Val372	vdWs
Tyr141-His214	π-π stacking	Trp369-Val372	H-bond
Tyr141-Gly215	vdWs	Trp369-Val373	H-bond
Tyr141-Trp468	π-π stacking	Asn370-Glu374	H-bond
Tyr141-Trp468	H-bond	Ser371-Ala375	H-bond
Tyr141-Trp468	vdWs	Ser371-Ala375	vdWs
Ile142-Gly215	H-bond	Val372-Ala376	H-bond
Ile142-Val216	vdWs	Val373-Trp377	H-bond
Ile142-Val216	vdWs	Glu374-Phe378	H-bond
Ile142-Leu217	H-bond	Glu374-Phe378	vdWs
Leu143-Leu217	vdWs	Ala375-Phe378	vdWs
Phe144-Phe151	π-π stacking	Ala375-Gly379	H-bond
Phe144-Leu217	H-bond	Ala375-Val380	H-bond
Ser146-Trp369	vdWs	Ala375-Val380	vdWs
Ser146-Asp390	H-bond	Ala376-Gly379	H-bond
Ser147-Met150	H-bond	Trp377-Arg448	π-cation
Ser147-Met150	H-bond	Trp377-Arg448	π-cation
Ser147-Met150	vdWs	Trp377-Arg448	H-bond
Ser147-Phe151	H-bond	Trp377-Arg448	vdWs
Ser147-Trp369	vdWs	Trp377-Ile451	vdWs
Ser147-Asn394	H-bond	Gly379-Ala440	vdWs
Ala148-Phe151	vdWs	Gly379-Ala440	vdWs
Ala148-Ser152	H-bond	Pro381-Arg437	vdWs
Ala148-Glu225	H-bond	Ile382-Trp403	H-bond
Thr149-Phe153	H-bond	Ile382-Val405	H-bond
Thr149-Phe153	vdWs	Gly384-Val405	H-bond
Thr149-Ser179	vdWs	Gly384-Val405	vdWs
Thr149-Ser228	H-bond	Gly384-Trp406	vdWs
Met150-Phe153	vdWs	Trp385-Trp410	π-π stacking
Met150-Phe154	H-bond	Trp385-Trp410	π-π stacking

Node-Node	Interaction	Node-Node	Interaction
Met150-Asp390	vdWs	Trp385-Trp410	vdWs
Phe151-Phe154	π-π stacking	Trp385-Ile423	vdWs
Phe151-Phe154	H-bond	Pro386-Gln391	vdWs
Phe151-Ala155	H-bond	Pro386-Lys392	vdWs
Phe151-Leu232	vdWs	Pro386-Lys392	vdWs
Ser152-Leu232	vdWs	Leu387-Gln391	H-bond
Ser152-Leu232	vdWs	Leu387-Glu413	H-bond
Phe153-Phe157	π-π stacking	Leu387-Glu413	vdWs
Phe153-Phe157	H-bond	His388-Gln391	H-bond
Phe153-Phe157	vdWs	His388-Gln391	H-bond
Phe153-Leu192	vdWs	His388-Gln391	vdWs
Phe154-Phe157	H-bond	His388-Trp412	vdWs
Phe154-Phe203	π-π stacking	Asp390-Ile393	H-bond
Phe154-Phe203	vdWs	Asp390-Ile393	vdWs
Phe154-Ser207	H-bond	Asp390-Ile393	vdWs
Tyr156-Leu160	H-bond	Asp390-Asn394	H-bond
Tyr156-Leu160	vdWs	Gln391-Asn394	H-bond
Tyr156-Ile175	vdWs	Gln391-Asn394	vdWs
Phe157-Leu160	H-bond	Gln391-Ala395	H-bond
Phe157-Leu160	vdWs	Lys392-Glu396	H-bond
Phe157-Ala161	H-bond	Lys392-Glu396	vdWs
Phe157-Phe166	π-π stacking	Lys392-Gly411	vdWs
Phe157-Tyr200	π-π stacking	Lys392-Trp412	π-cation
Phe157-Phe203	π-π stacking	Lys392-Trp412	vdWs
Phe157-Phe203	vdWs	Ile393-Glu396	vdWs
Phe157-Phe203	vdWs	Ile393-Val397	H-bond
Pro158-Lys162	vdWs	Ile393-Val397	vdWs
Pro158-Ser207	vdWs	Asn394-Val397	H-bond
Pro158-Ser207	vdWs	Asn394-Val398	H-bond
Thr159-Lys162	vdWs	Ala395-Val398	vdWs
Leu160-Ser163	H-bond	Ala395-Ala399	H-bond
Leu160-Phe166	vdWs	Glu396-Lys400	H-bond
Leu160-Phe166	vdWs	Glu396-Lys400	vdWs
Ser163-Phe166	H-bond	Glu396-Lys400	vdWs
Ser165-Lys169	H-bond	Glu396-Lys400	vdWs
Ser165-Lys169	vdWs	Glu396-Trp406	H-bond
Ser165-Leu170	H-bond	Glu396-Trp406	vdWs
Ser165-Leu170	vdWs	Val398-Gly401	H-bond
Ser165-Leu170	vdWs	Val398-Gly402	H-bond

Node-Node	Interaction	Node-Node	Interaction
Phe166-Leu193	vdWs	Ala399-Gly402	H-bond
Phe166-Tyr200	π-π stacking	Gly402-Leu436	vdWs
Pro167-Arg185	H-bond	Lys407-Trp410	H-bond
Asp171-Arg185	H-bond	Lys407-Trp410	vdWs
Asp171-Arg185	vdWs	Lys407-Trp410	vdWs
Phe172-Pro184	vdWs	Lys407-Glu429	Ionic bond
Phe172-Pro184	vdWs	Lys407-Glu429	H-bond
Val173-Ile183	H-bond	Gly409-Arg416	H-bond
Val173-Ile183	H-bond	Gly409-Arg416	vdWs
Val173-Ile183	vdWs	Trp410-Val418	vdWs
Ile175-Val178	vdWs	Trp412-Glu415	H-bond
Gly177-Glu227	vdWs	Trp412-Glu415	H-bond
Gly177-Ala231	vdWs	Trp412-Glu415	vdWs
Ser179-Glu227	vdWs	Trp412-Glu415	vdWs
Ser179-Ser228	H-bond	Trp412-Glu415	vdWs
Ser179-Ser228	H-bond	Arg416-Glu422	Ionic bond
Ser179-Ser228	vdWs	Arg416-Glu422	H-bond
Ser179-Ser228	vdWs	Arg416-Glu422	H-bond
Pro184-Ser187	H-bond	Lys419-Glu422	H-bond
Pro184-Ser187	vdWs	Lys419-Ile423	H-bond
Pro184-Ile188	vdWs	Gly420-Ala424	H-bond
Arg185-Ile188	H-bond	Glu421-Glu425	H-bond
Ser186-Lys392	H-bond	Glu421-Glu425	vdWs
Ser187-Trp412	vdWs	Glu421-Arg428	H-bond
Ile188-Trp412	vdWs	Glu422-Ala426	H-bond
Ile188-Trp412	vdWs	Glu422-Ala426	vdWs
Pro189-Leu192	H-bond	Ile423-Ala426	vdWs
Pro189-Leu192	vdWs	Ile423-Ile427	H-bond
Pro190-Leu193	H-bond	Ala424-Ile427	vdWs
Pro191-Asp194	H-bond	Ala424-Arg428	H-bond
Pro191-Asp194	vdWs	Glu425-Arg428	H-bond
Pro191-Ser197	H-bond	Glu425-Glu429	H-bond
Pro191-Phe199	vdWs	Ala426-Glu429	H-bond
Pro191-Phe199	vdWs	Ala426-Val430	H-bond
Asp194-Ser197	H-bond	Ala426-Val430	vdWs
Asp194-Ser197	vdWs	Ile427-Met431	H-bond
Asp194-Tyr200	vdWs	Ile427-Met431	vdWs
Pro195-Tyr200	vdWs	Arg428-Asn432	H-bond
Pro195-Tyr200	vdWs	Arg428-Asn432	vdWs

Node-Node	Interaction	Node-Node	Interaction
Ser197-Tyr200	vdWs	Val430-Asp433	H-bond
Ser197-Lys201	H-bond	Val430-Asp433	vdWs
Ser197-Lys201	vdWs	Met431-Arg437	H-bond
Leu198-Lys201	H-bond	Asp433-Leu436	vdWs
Leu198-Lys201	vdWs	Glu434-Arg437	vdWs
Leu198-Lys201	vdWs	Glu434-Arg437	vdWs
Leu198-Leu202	H-bond	Glu434-Met438	H-bond
Leu198-Leu202	vdWs	Ser435-Met438	vdWs
Phe199-Phe203	π-π stacking	Ser435-Lys439	H-bond
Phe199-Phe203	H-bond	Ser435-Lys439	vdWs
Phe199-Phe203	vdWs	Leu436-Lys439	vdWs
Tyr200-Met204	H-bond	Leu436-Ala440	H-bond
Tyr200-Met204	vdWs	Met438-Gln442	H-bond
Lys201-Glu205	H-bond	Lys439-Gln442	H-bond
Leu202-Asp206	H-bond	Lys439-Val443	H-bond
Phe203-Asp206	H-bond	Ala440-Val443	vdWs
Phe203-Ser207	H-bond	Ala440-Lys444	H-bond
Phe203-Ser207	vdWs	Thr441-Lys445	H-bond
Met204-Pro208	vdWs	Gln442-Lys445	H-bond
Glu205-Lys209	Ionic bond	Gln442-Lys445	vdWs
Glu205-Lys209	H-bond	Gln442-Asp446	H-bond
Asp206-Lys209	H-bond	Gln442-Asp446	vdWs
Ser207-Leu210	H-bond	Val443-Asp446	H-bond
Pro208-Lys211	vdWs	Val443-Ala447	H-bond
Lys209-Lys212	H-bond	Lys444-Ala447	H-bond
Leu210-Leu213	H-bond	Lys444-Arg448	H-bond
Leu210-Leu213	vdWs	Lys445-Arg448	vdWs
Lys211-Gly240	vdWs	Lys445-Lys449	H-bond
His214-Pro243	vdWs	Lys445-Lys449	vdWs
Val216-Pro243	H-bond	Lys445-Lys449	vdWs
Val218-Tyr245	H-bond	Asp446-Ala450	H-bond
Val218-Val247	H-bond	Ala447-Ala450	H-bond
Val218-Val247	vdWs	Arg448-Ser452	H-bond
Asn219-Phe250	H-bond	Lys449-Ser452	H-bond
Asn219-Phe250	vdWs	Ala450-Gln457	H-bond
Asn219-Trp369	H-bond	Ser452-Gly455	H-bond
Asn219-Trp369	vdWs	Ser452-Gly455	vdWs
Asn219-Val373	vdWs	Gly454-Glu458	H-bond
Thr220-Glu225	vdWs	Gly455-Val459	H-bond

Node-Node	Interaction	Node-Node	Interaction
Thr220-Leu229	vdWs	Ser456-Ala460	H-bond
Thr220-Gly248	H-bond	Gln457-Ala460	vdWs
Phe221-Ile224	H-bond	Gln457-Leu461	H-bond
Phe221-Ile224	vdWs	Gln457-Leu461	vdWs
Phe221-Glu225	H-bond	Glu458-Gln462	H-bond
Phe221-Glu225	vdWs	Val459-Lys463	H-bond
Phe221-Gly248	vdWs	Ala460-Leu464	H-bond
Phe221-Pro249	vdWs	Ala460-Leu464	vdWs
Glu222-Lys226	H-bond	Leu461-Leu464	H-bond
Glu222-Lys226	vdWs	Leu461-Met465	H-bond
Glu225-Leu229	H-bond	Gln462-Glu466	H-bond
Lys226-Leu229	vdWs	Gln462-Glu466	vdWs
Lys226-Glu230	Ionic bond	Leu464-Val467	H-bond
Lys226-Glu230	H-bond	Met465-Trp468	vdWs
Lys226-Glu230	vdWs	Met465-Lys469	H-bond
Glu227-Ala231	H-bond		

Table S16 The number of interactions between different edge types of WT and Mut10 based on overall network.

Interaction	WT	Mut10
H-bond	275	342
π-π stacking	19	23
π-cation	1	4
Ionic bond	7	7
π-H bond	3	3
vdWs	312	352
Total number	617	731

Table S17 List of primers for constructing mutants.

Primer	Sequence (5′ to 3′)
T49V-F	GACCCTGATTGTGCCGCAGCCGACCGTGAG
T49V-R	TCGGCTGCGGCACAATCAGGGTCACATGGCAATGCTG
T53P-F	GCAGCCGCCGGTGAGCAAAGCGGAAGAAGATCTGCTGA
T53P-R	TTGCTCACCGGCGGCTGCGGGGTAATCAGGGT
S110L-F	TGCTGCTGAGCCTGACCCCGCCGCTGAGCAGCTTTATTTATG
S110L-R	GGTCAGGCTCAGCAGCAGCGGGGTCAGCAGATGGCTA
S179F-F	TCCGGGCGTGTTTGTGAGCAGCATTCCACGCAG
S179F-R	ATGCTGCTCACAAACACGCCCGGAATTTCCACAAAATC
G200W-F	CCTGTTTTGGAAACTGTTTATGGAAGATAGCCCGA
G200W-R	AACAGTTTCCAAAACAGGCTGTTCGGCACC
S207A-F	ATGGAAGATGCGCCGAAACTGAAAAAACTGCATGGTGTGCT
S207A-R	TTCGGCGCATCTTCCATAAACAGTTTGCCAAACAGGCT
G246P-F	GGTGTATCCGGTGGGCCCGTTTGTGCCGTGCGAATTTG
G246P-R	ACGGGCCCACCGGATACACCGGCGGCAGGCCTTTAACCACT
V333W-F	CGAACTGTGGGAACGCATGGTGAAAGAAAAAAAAGGCCTG
V333W-R	ATGCGTTCCCACAGTTCGAAGCCTAACACGCCGTCCA
Q51I-F	TACCCCGATTCCGACCGTGAGCAAAGC
Q51I-R	ACGGTCGGAATCGGGGTAATCAGGGTCACA
S274P-F	AACAGCCGCCGGGCAGCGTGGTGTATGTGAG
S274P-R	ACGCTGCCCGGCGGCTGTTCATCCAGCCATTC
C253F-F	GTGCCGTTTGAATTTGAAAAAGTGGTGAAACGCGGCGA
C253F-R	CTTTTTCAAATTCAAACGGCACAAACGGGCCCAC
F330P-F	GTTAGGCCCGGAACTGGTGGAACGCATGGT
F330P-R	ACCAGTTCCGGGCCTAACACGCCGTCCA
G200Y-F	CCTGTTTTATAAACTGTTTATGGAAGATAGCCCGA
G200Y-R	AACAGTTTATAAAACAGGCTGTTCGGCACC
G200T-F	CCTGTTTACGAAACTGTTTATGGAAGATAGCCCGA
G200T-R	AACAGTTTCGTAAACAGGCTGTTCGGCACC
T106H-F	TCTGCTGCATCCGCTGCTGAGCAGCCTGAC
T106H-R	AGCAGCGGATGCAGCAGATGGCTACTGCTGCGA
E339K-F	GGTGAAAAAGAAAAAAGGCCTGGTGGTTAAAGAATGG
E339K-R	CCTTTTTTCTTTTTCACCATGCGTTCCACCAG
E339L-F	GGTGAAACTGAAAAAAGGCCTGGTGGTTAAAGAATGG
E339L-R	CCTTTTTTCAGTTTCACCATGCGTTCCACCAG
V467M-F	TGATGGAAATGTGGAAAAAAAACGTGCTCGAGCACC
V467M-R	CGTTTTTTTTCCACATTTCCATCAGTTTCTGCAGCGCCA
V467S-F	TGATGGAAAGCTGGAAAAAAAACGTGCTCGAGCACC
V467S-R	CGTTTTTTTTCCAGCTTTCCATCAGTTTCTGCAGCGCCA

Primer	Sequence (5′ to 3′)
V333L-F	CGAACTGCTGGAACGCATGGTGAAAGAAAAAAAAGGCCTG
V333L-R	ATGCGTTCCAGCAGTTCGAAGCCTAACACGCCGTCCA
G246C-F	GGTGTATTGCGTGGGCCCGTTTGTGCCGTGCGAATTTG
G246C-R	ACGGGCCCACGCAATACACCGGCGGCAGGCCTTTAACCACT
V194D-F	CACTGCTGGATCCGAACAGCCTGTTTGGCAAACT
V194D-R	TGTTCGGATCCAGCAGTGGCGGCGGAA
V194N-F	CACTGCTGAATCCGAACAGCCTGTTTGGCAAACT
V194N-R	TGTTCGGATTCAGCAGTGGCGGCGGAA
V437R-F	AGCCTGCGCATGAAAGCGACCCAAGTGAAAAAAGAT
V437R-R	TCGCTTTCATGCGCAGGCTTTCATCGTTCATCACTTCG
S100R-F	GCATTCGCCGCAGTAGCCATCTGCTGACCCCGCT
S100R-R	TGGCTACTGCGGCGAATGCTCGCAAACTGCAGAAAAAACG
L227E-F	GCATTGAAAAAGAGAGCCTGGAAGCGCTGAACG
L227E-R	CAGGCTCTCTTTTTCAATGCCTTCAAAGGTGTTCACCAGC
L227R-F	GCATTGAAAAACGGAGCCTGGAAGCGCTGAACG
L227R-R	CAGGCTCCGTTTTTCAATGCCTTCAAAGGTGTTCACCAGC
K445E-F	GCAAAGAAATTAGCGTGGGCGGTGGCT
K445E-R	CCACGCTAATTTCTTTGCGCGCATCTTTTTTCACTTGGGTC
K381P-F	TGGCGTGCCAATTCTGGGCTGGCCGCTGCAT
K381P-R	AGCCCAGAATTGGCACGCCAAACCACGCCGCT
G289S-F	ACCGCGATGAGCCGCGAACAGCTGCGCGAAGT
G289S-R	TTCGCGGCTCATCGCGGTGCGGCTGCCAAAG
D446E-F	GACCCAAGTGAAAAAAGAAGCGCGCAAAGCGATTAGC
D446E-R	TTGCGCGCTTCTTTTTTCACTTGGGTCGCTTTCATCACC
M438E-F	GAAAGCCTGGTGGAAAAAGCGACCCAAGTGAAAAAAGATG
M438E-R	GGTCGCTTTTTCCACCAGGCTTTCATCGTTCATCAC
E59S-F	CAAAGCGGAAAGCGATCTGCTGAGCCGCTTTCTG
E59S-R	AGCAGATCGCTTTCCGCTTTGCTCACGGTC
H214D-F	GAAAAAACTGGATGGTGTGCTGGTGAACACCTT
H214D-R	CACACCATCCAGTTTTTTCAGTTTCGGGCTATCTTCCA
H140C-F	TGCCGTGCTATATTCTGTTTACGAGCAGCGCGACCATG
H140C-R	AACAGAATATAGCACGGCACGCCCAGGCTT
V296L-F	TGCGCGAACTGGGCGATGGCCTGGTGAAAAGCGGCT
V296L-R	ATCGCCCAGTTCGCGCAGCTGTTCGCGGCCCA
V296I-F	TGCGCGAAATTGGCGATGGCCTGGTGAAAAGCGGCT
V296I-R	ATCGCCAATTTCGCGCAGCTGTTCGCGGCCCA
T106Y-F	AGTAGCCATCTGCTGTATCCGCTGCTGAGCA
T106Y-R	GATACAGCAGATGGCTACTGCTGCGAATGCTCG
T106A-F	CATCTGCTGGCGCCGCTGCTGAGCAGCCT

Primer	Sequence (5′ to 3′)
T106A-R	AGCGGCGCCAGCAGATGGCTACTGCTGCGAATG
D411G-F	GAAAGAAGGCTGGGGCTGGGAAGGCGAA
D411G-R	AGCCCCAGCCTTCTTTCCACACGCCCCA
S118A-F	GAGCGCGTTTATTTATGATATGACGCTGATTAGCCCGCT
S118A-R	CATAAATAAACGCGCTCAGCGGCGGGGTCA
G456S-F	TGGGCGGTAGCTGCGAAGTGGCGCTGCA
G456S-R	TCGCAGCTACCGCCCACGCTAATCGCT
H140T-F	TGCCGACCTATATTCTGTTTACGAGCAGCGCGA
H140T-R	CAGAATATAGGTCGGCACGCCCAGGCTTTC
Q51V-F	TACCCCGGTGCCGACCGTGAGCAAAGCGGAAG
Q51V-R	ACGGTCGGCACCGGGGTAATCAGGGTCACATGGCA
E415V-F	TTGGGAAGGCGTGCGCCTGGTGAAAGGCGAAGAAATTG
E415V-R	AGGCGCACGCCTTCCCAATCCCAGCCTTC
K211P-F	CGAAACTGCCGAAACTGCATGGTGTGCTGGT
K211P-R	GCAGTTTCGGCAGTTTCGGGCTATCTTCCATAAACAGT
K346N-F	CTGGTGGTTAACGAATGGGTGGATCAGAGCGAA
K346N-R	CACCCATTCGTTAACCACCAGGCCTTTTTTTTCTTTC
V180P-F	CGTGAGCCCGAGCAGCATTCCACGCAGCA
V180P-R	ATGCTGCTCGGGCTCACGCCCGGAATTTCCA
V259P-F	TGAAAAAGTGCCGAAACGCGGCGAAACCATTAGC
V259P-R	CGTTTCGGCACTTTTTCAAATTCGCACGGCAC
C457Q-F	GGTGGCCAAGAAGTGGCGCTGCAGAAACT
C457Q-R	CCACTTCTTGGCCACCGCCCACGCTAATC
V459Q-F	TGGCTGCGAACAAGCGCTGCAGAAACTGATGGAAGTGT
V459Q-R	CAGCGCTTGTTCGCAGCCACCGCCCACGCTAATC
E458K-F	GTGGCTGCAAAGTGGCGCTGCAGAAACTGATGGA
E458K-R	AGCGCCACTTTGCAGCCACCGCCCACGCTAATC
G424A-F	AGAAATTGCGGAAGCGATTCGCGAAGTGATGA
G424A-R	ATCGCTTCCGCAATTTCTTCGCCTTTCACCAGG
S97A-F	GTTTGCGGCGATTCGCAGCAGTAGCCATCTG
S97A-R	GCTGCGAATCGCCGCAAACTGCAGAAAAAACGGAT
F172V-F	GCAAACTGGATGTGGTGGAAATTCCGGGCGTGAG
F172V-R	TTCCACCACATCCAGTTTGCCCGGAAAGCT
S163D-F	CTGGCGAAAGATGAAAGCTTTCCGGGCAAACTG
S163D-R	AAGCTTTCATCTTTCGCCAGGGTCGGAAAATAGC
L227E-F	GGCATTGAAAAAGAAAGCCTGGAAGCGCTGAACG
L227E-R	AGGCTTTCTTTTTCAATGCCTTCAAAGGTGTTCACCAGC
F330E-F	GTGTTAGGCGAAGAACTGGTGGAACGCATGGT
F330E-R	CAGTTCTTCGCCTAACACGCCGTCCAG

Primer	Sequence (5′ to 3′)
T264A-F	CGAAGCGATTAGCGAATGGCTGGATGAACAGCCGA
T264A-R	TTCGCTAATCGCTTCGCCGCGTTTCACCACTTTTTCAA
D313A-F	GGTGAAAGCGAAAATTGTGGATCGCGCGGAAGAG
D313A-R	CAATTTTCGCTTTCACCACCCACAGAAAGCGCCA
S155A-F	GTTTAGCTTTTTTGCGTATTTTCCGACCCTGGCGAA
S155A-R	TACGCAAAAAAGCTAAACATGGTCGCGCT
S274A-F	GAACAGCCGGCGGGCAGCGTGGTGTATGTGA
S274A-R	CTGCCCGCCGGCTGTTCATCCAGCCAT
H40E-F	GTTACTGGAACAGCATTGCCATGTGACCCT
H40E-R	CAATGCTGTTCCAGTAACAGGCTCGCCAGG
S22N-F	TGTTACCGAACGCCGGCATGGGCCAT
S22N-R	TGCCGGCGTTCGGTAACAGCGCCACATGC
S36A-F	TGGCGGCGCTGTTACTGCATCAGCATTGCCAT
S36A-R	GCAGTAACAGCGCCGCCAGGCGCAGAAAC
D446S-F	GAAAAAAAGCGCGCGCAAAGCGATTAGCGT
D446S-R	TGCGCGCGCTTTTTTTCACTTGGGTCGCTTTCATCACC
L129M-F	AGCCCGATGCTGCCGATTGCGGAAAGC
L129M-R	TCGGCAGCATCGGGCTAATCAGCGTCATATCAT
L104N-F	GTAGCCATAACCTGACCCCGCTGCTGAGCA
L104N-R	GGTCAGGTTATGGCTACTGCTGCGAATGCTCG
S181D-F	GTGAGCGTGGATAGCATTCCACGCAGCAGCAT
S181D-R	ATGCTATCCACGCTCACGCCCGGAATTTC
R290K-F	ATGGGCAAAGAACAGCTGCGCGAAGTGG
R290K-R	AGCTGTTCTTTGCCCATCGCGGTGC
S187C-F	CCACGCAGCTGCATTCCGCCGCCACTGCT
S187C-R	GGAATGCAGCTGCGTGGAATGCTGCTCACGCT
T441S-F	ATGAAAGCGAGCCAAGTGAAAAAAGATGCGCGCAAAG
T441S-R	ACTTGGCTCGCTTTCATCACCAGGCTTTCAT
E267K-F	CCATTAGCAAATGGCTGGATGAACAGCCGAG
E267K-R	CAGCCATTTGCTAATGGTTTCGCCGCGTT
S165D-F	GAAAAGCGAAGATTTTCCGGGCAAACTGGATTTTGTGG
S165D-R	GAAAATCTTCGCTTTTCGCCAGGGTCG
S111N-F	TGCTGAGCAACCTGACCCCGCCGCTGAGCAGCTT
S111N-R	GGTCAGGTTGCTCAGCAGCGGGGTCAGCAGA
S102A-F	CAGCAGTGCGCATCTGCTGACCCCGCTG
S102A-R	GCAGATGCGCACTGCTGCGAATGCTCGCA
K201S-F	TTGGCAGCCTGTTTATGGAAGATAGCCCGAAACTGA
K201S-R	CATAAACAGGCTGCCAAACAGGCTGTTCGG
T106L-F	ATCTGCTGCTGCCGCTGCTGAGCAGCCTGA

Primer	Sequence (5′ to 3′)
T106L-R	CAGCGGCAGCAGCAGATGGCTACTGCTGCGA
C43N-F	TCAGCATAACCATGTGACCCTGATTACCCCGCA
C43N-R	TCACATGGTTATGCTGATGCAGTAACAGGCTCG
V238T-F	GCAAAGTGACCAAAGGCCTGCCGCCGGT
V238T-R	CCTTTGGTCACTTTGCCGCCGTTCAGCGCT
E353L-F	TCAGAGCCTGATTCTGGGCCATAAAGCGGTG
E353L-R	CCAGAATCAGGCTCTGATCCACCCATTCTTTAACCAC